We are IntechOpen, the world's leading publisher of Open Access books Built by scientists, for scientists

4,800
Open access books available

122,000
International authors and editors

135M
Downloads

Our authors are among the

154
Countries delivered to

TOP 1%
most cited scientists

12.2%
Contributors from top 500 universities

CLARIVATE ANALYTICS BOOK CITATION INDEX INDEXED

WEB OF SCIENCE™

Selection of our books indexed in the Book Citation Index in Web of Science™ Core Collection (BKCI)

Interested in publishing with us?
Contact book.department@intechopen.com

Numbers displayed above are based on latest data collected.
For more information visit www.intechopen.com

2

Topological Singularities in Acoustic Fields due to Absorption of a Crystal

V. I. Alshits[1,2], V. N. Lyubimov[1] and A. Radowicz[3]
[1]*A.V. Shubnikov Institute of Crystallography, Russian Academy of Sciences, Moscow,*
[2]*Polish-Japanese Institute of Information Technology, Warsaw,*
[3]*Kielce University of Technology, Kielce*
[1]*Russia*
[2,3]*Poland*

1. Introduction

The influence of energy dissipation on the properties of bulk elastic waves in crystals is not at all reduced to trivial decrease in their amplitudes along propagation. In anisotropic media the situation is much more complicated than it looks like at first glance, at least for such specific directions of propagation as acoustic axes. The latter are defined as directions $\mathbf{m}_0$ along which a degeneracy of the phase speeds of two isonormal waves occurs (Fedorov, 1968; Khatkevich, 1962a, 1964). The corresponding points of the contact of the degenerate sheets of the phase velocity surface P may be tangent or conical (Alshits & Lothe, 1979; Alshits, Sarychev & Shuvalov, 1985) (Fig.1).

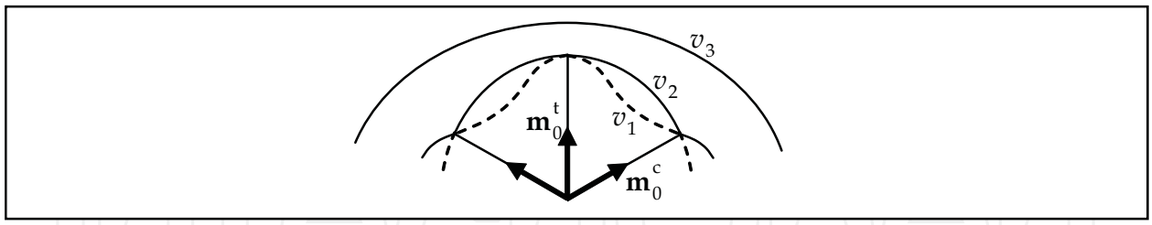

Fig. 1. Schematic plot of the section fragment of the three sheets of the phase velocity surface $v_\alpha(\mathbf{m})$ ($\alpha = 1, 2, 3$) containing one tangent and two conical points of degeneracy

Taking into account that formally the wave attenuation may be described as an imaginary perturbation of the phase speed, one could expect due to the damping either a shift or a split of the acoustic axis, of course if it is not created by a symmetry. As we shall see below, for an acoustic axis of general position it is just splitting what is realized, and with quite a radical transformation of the local geometry of the phase velocity surface. The other possible reason for sensitivity of the wave properties to a small attenuation is related to a polarization aspect. Indeed, it is known (Alshits & Lothe, 1979; Alshits, Sarychev & Shuvalov, 1985) that the acoustic axes indicate on the unit sphere of propagation directions $\mathbf{m}^2 = 1$ the singular points in the vector fields of polarizations which are characterized by the definite vector

rotation around these points on $\pm 2\pi$ or $\pm\pi$, i.e. by the Poincarè indices $n = \pm 1$ or $\pm 1/2$ (Fig.2). It is clear that a split of such singular points must be quite catastrophic for the corresponding polarization distribution. And that really occurs.

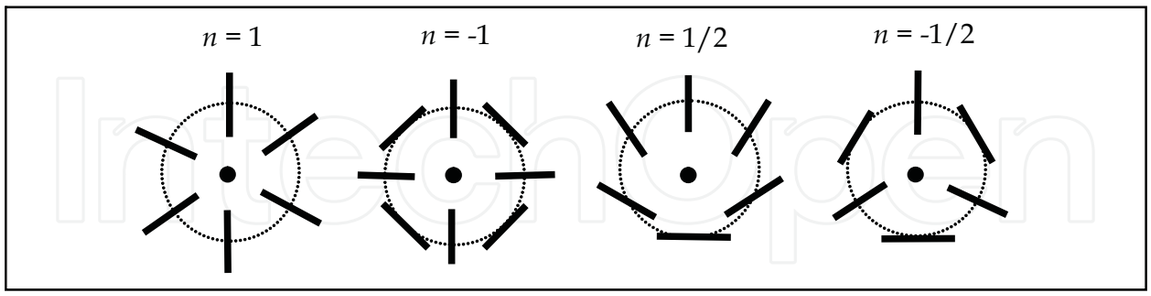

Fig. 2. Singular polarization distributions around the two types of tangent degeneracy points $n=\pm 1$ and the two types of conical degeneracies $n=\pm 1/2$

The above peculiarities are associated with space distribution of wave characteristic rather than with individual properties of bulk elastic waves. Meanwhile, as we shall see, in absorptive crystals the individual wave properties close to degeneracy directions also manifest quite unusual features, such as an almost circular polarization, in contrast to a quasi-linear one in the non-degenerate regions.

The theory of acoustic axes in non-absorptive anisotropic media is quite complete. For a review we address readers to the paper by Shuvalov (1998). The theory gives the general criteria of the degeneracy occurrence and describes all possible types of acoustic axes classifying them with respect to a local geometry of the degenerate velocity sheets and to specific features of the vector polarization fields around the degeneracy directions. This classification (Alshits & Lothe, 1979; Alshits, Sarychev & Shuvalov, 1985) includes more types than we presented in Figs. 1 and 2. However, apart from a line degeneracy known in hexagonal crystals, the rest additional types relate to the model media with accidentally coinciding or vanishing material constants (or some their combinations). Such media are beyond our interest in this paper. Note in addition that conical acoustic axes may exist in real crystals even in quite non-symmetric directions and always exist along the symmetry axis *3*. In contrast, tangent degeneracies are realized in practice only due to a high symmetry of the crystals and are known only along symmetry axes ∞ and *4*. As was shown in (Alshits & Lothe, 1979; Alshits, Sarychev & Shuvalov, 1985) , all the "model" acoustic axes together with any tangent or line degeneracies are unstable and must disappear, split or be transformed into other types under any small triclinic perturbation of the elastic moduli tensor $\hat{c}$. The only stable type of acoustic axes is the conical type. Under any real perturbation $\delta\hat{c}$ a conical degeneracy never split or disappear, but can only shift.

The wave attenuation can be interpreted as a perturbation of the tensor $\hat{c}$, however not real but imaginary. As was mentioned in (Alshits, Sarychev & Shuvalov, 1985), under such a non-hermitian perturbation even a conical degeneracy may lose its stability. Later Shuvalov & Chadwick (1997) rigorously investigated the stability of different acoustic axes with respect to a weak thermoelastic coupling. Their conclusion was: all types of degeneracies are unstable including a conical acoustic axis which splits into a pair. The same problem for viscoelastic and thermo-viscoelastic media has been studied by Shuvalov & Scott (1999, 2000) with similar conclusions.

It is evident that the considered physical mechanisms of the damping definitely do not disturb symmetry of the crystal and therefore cannot shift or split degeneracies along symmetry axes ∞, *4* and *3*. It means that any really existing tangent degeneracies and conical degeneracies along symmetry axes *3* must be stable under the damping perturbation. This statement was proved by Alshits & Lyubimov (1998) for viscoelastic media.

In this chapter we shall consider the attenuation in terms of viscoelasticity following to the approach of the papers (Alshits & Lyubimov, 1998, 2011). We shall analyse in detail the mentioned above geometrical peculiarities and polarization singularities related to a pair of the so-called singular acoustic axes representing a new type of stable degeneracy and arising as a result of the considered split of a conical acoustic axis. On this basis we shall develop an extension of the classical theory of internal conical refraction (Barry & Musgrave, 1979; De Klerk & Musgrave, 1955; Fedorov, 1968; Khatkevich, 1962b; Musgrave, 1957) for an absorptive crystal. As will be shown, the damping provides very radical and non-trivial modifications of fundamental features of the phenomenon.

2. Statement of the problem and general relations

Let us consider the viscoelastic medium characterized by the density ρ and the tensors of elastic moduli $\hat{c}$ and viscosity $\hat{\eta}$. The dynamic displacement field $\mathbf{u}(\mathbf{r},t)$ in such medium is described by the known equation (Landau & Lifshitz, 1986)

$$\rho\ddot{u}_i = c_{ijkl}u_{l,kj} - \eta_{ijkl}\dot{u}_{l,kj}\,, \tag{1}$$

where the vectors $\dot{\mathbf{u}}$ and $\ddot{\mathbf{u}}$ are the velocity and acceleration fields and the usual notation $...,_k \equiv \partial / \partial x_k ...$ is accepted. For the bulk wave

$$\mathbf{u}(\mathbf{r},t) = C\mathbf{A}\exp[ik(\mathbf{m}\cdot\mathbf{r} - vt)] \tag{2}$$

propagating along the wave vector $\mathbf{k} = k\mathbf{m}$ with the amplitude *C*, the frequency $\omega = kv$, the phase speed *v* and the polarization **A**, eqn. (1) is transformed into Christoffel`s equation

$$(\hat{Q}' - i\hat{Q}'')\mathbf{A} = \rho v^2\mathbf{A} \tag{3}$$

where $\hat{Q}'$ and $\hat{Q}''$ are the real symmetric matrices

$$Q'_{jk} = m_i c_{ijkl} m_l\,, \qquad Q''_{jk} = \omega m_i \eta_{ijkl} m_l\,. \tag{4}$$

Note, that the imaginary addition $-i\hat{Q}''$ to the usual acoustic tensor $\hat{Q}'$, in contrast to the latter, is dependent on the frequency. Eqn. (3) determines the three complex eigenvectors $\mathbf{A}_a$ and the three corresponding complex eigenvalues ρv_a^2 (α = 1, 2, 3), i.e. the three phase speeds v_a as functions of the direction **m**:

$$\mathbf{A}_a = \mathbf{A}'_a + i\mathbf{A}''_a\,, \qquad v_a = v'_a - iv''_a\,. \tag{5}$$

Below the frequency will be supposed to be real. Hence, by (5), the value k_a should contain an imaginary addition determining the decay of the wave along its propagation:

$$k_a \equiv k'_a + ik''_a = \frac{\omega}{v'_a - iv''_a} \approx \frac{\omega}{v'_a}\left(1 + i\frac{v''_a}{v'_a}\right). \tag{6}$$

The complex phase speeds of eigenwaves are found from the equation

$$\rho v_a^2 = \frac{\mathbf{A}_a(\hat{Q}' - i\hat{Q}'')\mathbf{A}_a}{\mathbf{A}_a \cdot \mathbf{A}_a}. \tag{7}$$

The polarization vectors $\mathbf{A}_a$ as eigenvectors of the symmetric matrix $\hat{Q}' - i\hat{Q}''$ for non-degenerate directions $\mathbf{m}$ of propagation must be mutually orthogonal

$$\mathbf{A}_a \cdot \mathbf{A}_\beta = \delta_{a\beta}, \qquad a \neq \beta. \tag{8}$$

As regards to their normalization, we cannot use the customary condition $\mathbf{A}_a^2 = 1$, bearing in mind the possibility of a circular polarization for which $\mathbf{A}_a^2 = 0$. Instead, the normalizing factor will be chosen so that

$$|\mathbf{A}_a|^2 = \mathbf{A}_a'^2 + \mathbf{A}_a''^2 = 1. \tag{9}$$

For a further development let us divide the basic eqn. (3) on the real and imaginary parts

$$\begin{aligned} \hat{Q}'\mathbf{A}'_a + \hat{Q}''\mathbf{A}''_a &= \rho(v_a'^2 - v_a''^2)\mathbf{A}'_a + 2\rho v'_a v''_a \mathbf{A}''_a, \\ \hat{Q}'\mathbf{A}''_a - \hat{Q}''\mathbf{A}'_a &= \rho(v_a'^2 - v_a''^2)\mathbf{A}''_a - 2\rho v'_a v''_a \mathbf{A}'_a. \end{aligned} \tag{10}$$

Multiplying these equations by $\mathbf{A}'_{a,\beta}$ or $\mathbf{A}''_{a,\beta}$ $(\alpha \neq \beta)$ and combining the results one obtains

$$2\rho v'_a v''_a = \mathbf{A}'_a \cdot \hat{Q}''\mathbf{A}'_a + \mathbf{A}''_a \cdot \hat{Q}''\mathbf{A}''_a, \tag{11}$$

$$\rho(v_a'^2 - v_a''^2) = \mathbf{A}'_a \cdot \hat{Q}'\mathbf{A}'_a + \mathbf{A}''_a \cdot \hat{Q}'\mathbf{A}''_a, \tag{12}$$

$$\rho(v_\beta'^2 - v_a'^2 + v_a''^2 - v_\beta''^2)\mathbf{A}''_a \cdot \mathbf{A}'_\beta = \mathbf{A}'_a \cdot \hat{Q}''\mathbf{A}'_\beta + \mathbf{A}''_a \cdot \hat{Q}''\mathbf{A}''_\beta - 2\rho(v'_a v''_a + v'_\beta v''_\beta)\mathbf{A}''_a \cdot \mathbf{A}''_\beta. \tag{13}$$

Eqns. (11)-(13) are exact. The first two of them show that the imaginary part of the phase speed v''_a being linear in small viscosity $\hat{\eta}$ is small compared to v'_a independently of the direction $\mathbf{m}$. In accordance with Eqn. (13), one can also conclude that $A''_a << A'_a$ however not for any $\mathbf{m}$, but only far enough from acoustic axes, when the difference $v'_\beta - v'_a$ is not small. In this case the value $A''_a = |\mathbf{A}''_a|$ is also linear in $\hat{\eta}$ and therefore small. Let us decompose the vector $\mathbf{A}''_a$ on the two components: $\mathbf{A}''_a = \mathbf{A}''^{\perp}_a + \mathbf{A}''^{\parallel}_a$, where $\mathbf{A}''^{\perp}_a \perp \mathbf{A}'_a$ and $\mathbf{A}''^{\parallel}_a \parallel \mathbf{A}'_a$. Thus, the ellipticity $\varepsilon = A''^{\perp}_a / A'_a$ of the wave polarization due to the damping is also small almost everywhere beyond small domains around acoustic axes. Let us estimate this ellipticity to the first order in $\hat{\eta}$.

Being perpendicular to $\mathbf{A}'_a$, the vector $\mathbf{A}''^{\perp}_a$ may be expressed in leading approximation as a superposition of two isonormal vectors $\mathbf{A}'_\beta$ and $\mathbf{A}'_\gamma$ which are almost orthogonal to $\mathbf{A}'_a$,

$$\mathbf{A}''^{\perp}_a \approx (\mathbf{A}''^{\perp}_a \cdot \mathbf{A}'_\beta)\mathbf{A}'_\beta + (\mathbf{A}''^{\perp}_a \cdot \mathbf{A}'_\beta)\mathbf{A}'_\beta \approx (\mathbf{A}''_a \cdot \mathbf{A}'_\beta)\mathbf{A}'_\beta + (\mathbf{A}''_a \cdot \mathbf{A}'_\beta)\mathbf{A}'_\beta. \tag{14}$$

In view of eqn. (13) this gives far from degeneracies

$$\mathbf{A}''^{\perp}_a = \frac{\mathbf{A}'_a \cdot \hat{Q}'' \mathbf{A}'_\beta}{\rho(v'^2_\beta - v'^2_a)} \mathbf{A}'_\beta + \frac{\mathbf{A}'_a \cdot \hat{Q}'' \mathbf{A}'_\gamma}{\rho(v'^2_\gamma - v'^2_a)} \mathbf{A}'_\gamma \,. \tag{15}$$

In fact, for considered non-singular directions the component $\mathbf{A}''^{\parallel}_a$ is physically unimportant. Indeed, the vector amplitude of the wave (2) in the accepted linear approximation is equal

$$C\mathbf{A}_a = C(\mathbf{A}'_a + i\mathbf{A}''^{\parallel}_a + i\mathbf{A}''^{\perp}_a) = C(1+i\varepsilon^{\parallel})\left(\mathbf{A}'_a + \frac{i\mathbf{A}''^{\perp}_a}{1+i\varepsilon^{\parallel}}\right) \approx C'(\mathbf{A}'_a + i\mathbf{A}''^{\perp}_a)\,, \tag{16}$$

where the notations $\varepsilon^{\parallel} = A''^{\parallel}_a / A'_a$ and $C' = C(1+i\varepsilon^{\parallel})$ are introduced.
With (15) and (9), the wave ellipticity is readily estimated as $\varepsilon \approx A''^{\perp}_a = |\mathbf{A}''^{\perp}_a|$. For similar non-singular directions the speeds v''_a and v'_a determined by eqns. (11) and (12) may be expressed in the same leading approximation as

$$v''_a = \frac{\mathbf{A}'_a \cdot \hat{Q}'' \mathbf{A}'_a}{2\rho v'_a}\,, \qquad \rho v'^2_a = \mathbf{A}'_a \cdot \hat{Q}' \mathbf{A}'_a\,. \tag{17}$$

On the other hand, eqn. (15) demonstrates the tendency to increasing ellipticity ε when the wave normal $\mathbf{m}$ approaches the degeneracy direction ($v'_a = v'_\beta$ or $v'_a = v'_\gamma$) and one of the denominators in (15) decreases becoming singular. Of course, in the vicinity of the degeneracy it is necessary to replace eqns. (15) and (17) by some other relations.

3. General formalism for the neighbourhood of an acoustic axis

In fact, eqns. (15) and (17) quite hold for the description of the non-degenerate wave branch even along the direction where two other branches are degenerate. In the further development we shall choose for the non-degenerate wave characteristics the number $a = 3$. In this notation, by eqn. (15), the vector $\mathbf{A}''_3$ must be small addition to $\mathbf{A}'_3$. In view of the orthogonality condition (8) this allows us in the leading approximation to replace the complex polarization vectors $\mathbf{A}_{1,2}$ by their projections on the plane orthogonal to the vector $\mathbf{A}'_3$. This must work even close to acoustic axes where the imaginary components of $\mathbf{A}_{1,2}$ might be comparable in the length with their real counterparts. We are following here the ideology developed in the theory of acoustic axes for the case of zero damping (Alshits & Lothe, 1979; Alshits, Sarychev & Shuvalov, 1985).
Thus, let $\mathbf{m}_0$ is the direction of the acoustic axis in the crystal with the "switched off" attenuation. By definition, along $\mathbf{m}_0$ there must be $v_1 = v_2 \equiv v_0$ and, apart from the non-degenerate wave with the speed v_3 and the polarization $\mathbf{A}_{03}$, any polarization in the degeneracy plane $D \perp \mathbf{A}_{03}$ is permissible (Fig.3).
Let us choose in the D plane an arbitrary pair of unit orthogonal vectors $\mathbf{A}_{01}$ and $\mathbf{A}_{02}$ forming with $\mathbf{A}_{03}$ the orthonormal right-handed basis $\{\mathbf{A}_{01}, \mathbf{A}_{02}, \mathbf{A}_{03}\}$ (Fig. 3).
Now "switch on" the damping and consider eqn. (3) close to $\mathbf{m}_0$ at $\mathbf{m} = \mathbf{m}_0 + \delta\mathbf{m}$:

$$(\mathbf{m}_0 + \delta\mathbf{m})(\hat{c} - i\omega\hat{\eta})(\mathbf{m}_0 + \delta\mathbf{m})\mathbf{A}_a = \rho(v_{0a} + \delta v_a)^2\mathbf{A}_a\,. \tag{18}$$

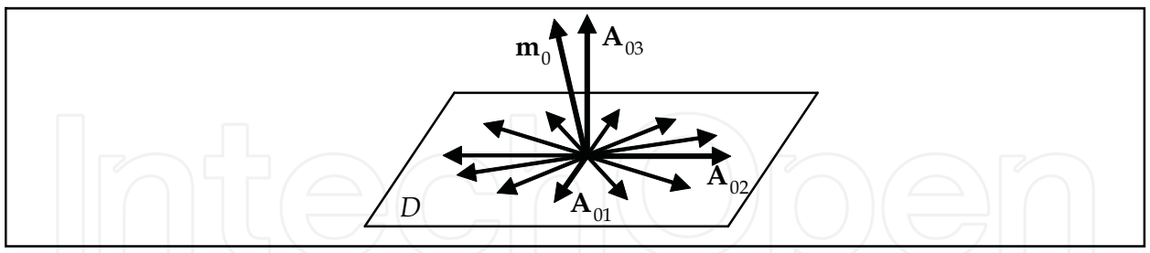

Fig. 3. Allowed polarizations along the acoustic axis $\mathbf{m}_0$ at "switched off" attenuation

In the linear approximation eqn. (18) is transformed to

$$(\hat{Q}_0 + \delta\hat{Q})\mathbf{A}_a = \rho(v_{0a}^2 + 2v_{0a}\delta v_a)\mathbf{A}_a\,, \tag{19}$$

where

$$\hat{Q}_0 = \hat{Q}'(\mathbf{m}_0)\,, \qquad \delta\hat{Q} = \mathbf{m}_0\hat{c}\delta\mathbf{m} + \delta\mathbf{m}\hat{c}\mathbf{m}_0 - i\hat{Q}_0''\,, \qquad \hat{Q}_0'' = \hat{Q}''(\mathbf{m}_0)\,. \tag{20}$$

The complex polarization vectors $\mathbf{A}_a$ may be decomposed in the basis $\{\mathbf{A}_{01}, \mathbf{A}_{02}, \mathbf{A}_{03}\}$ as

$$\mathbf{A}_a = a_{a\beta}\mathbf{A}_{0\beta}\,, \tag{21}$$

where $a, \beta = 1, 2, 3$ and the summation over β is assumed. Substituting the linear superpositions (21) at $a = 1$ and $a = 2$ into eqn. (19) one obtains

$$\begin{aligned} \delta\hat{Q}\mathbf{A}_1 &= 2\rho v_0\delta v_1\mathbf{A}_1 + \rho(v_0^2 - v_{03}^2)a_{13}\mathbf{A}_{03}\,, \\ \delta\hat{Q}\mathbf{A}_2 &= 2\rho v_0\delta v_2\mathbf{A}_2 + \rho(v_0^2 - v_{03}^2)a_{23}\mathbf{A}_{03}. \end{aligned} \tag{22}$$

Eqns. (22) show that the coefficients a_{13} and a_{23} must be linearly small. So, indeed in the leading approximation one can replace the polarization vectors $\mathbf{A}_1$ and $\mathbf{A}_2$ by their projections on the D-plane

$$\mathbf{A}_1 \approx a_{11}\mathbf{A}_{01} + a_{12}\mathbf{A}_{02}\,, \qquad \mathbf{A}_2 \approx a_{21}\mathbf{A}_{01} + a_{22}\mathbf{A}_{02}\,. \tag{23}$$

Multiplying eqns. (22) by $\mathbf{A}_1$ or $\mathbf{A}_2$ we obtain the two linear systems determining the coefficients $a_{a\beta}$ in (23):

$$\begin{cases} (\delta Q_{11} - 2v_0\rho\delta v_1)a_{11} + \delta Q_{12}a_{12} = 0, \\ \delta Q_{12}a_{11} + (\delta Q_{22} - 2v_0\rho\delta v_1)a_{12} = 0; \end{cases} \qquad \begin{cases} (\delta Q_{11} - 2v_0\rho\delta v_2)a_{21} + \delta Q_{12}a_{22} = 0, \\ \delta Q_{12}a_{21} + (\delta Q_{22} - 2v_0\rho\delta v_2)a_{22} = 0; \end{cases} \tag{24}$$

where

$$\delta Q_{ij} = \mathbf{A}_{0i}\cdot\delta\hat{Q}\mathbf{A}_{0j}\,, \qquad i, j = 1, 2\,. \tag{25}$$

The conditions for the existence of nontrivial solutions of the systems (24) give the common quadratic equation determining both δv_1 and δv_2

$$(\delta Q_{11} - 2v_0\rho\delta v)(\delta Q_{22} - 2v_0\rho\delta v) - \delta Q_{12}^2 = 0 \tag{26}$$

with the roots determining the unknown additions $\delta v_{1,2}$ to the degenerate speed v_0:

$$\delta v_{1,2} = \mathbf{s}_0 \cdot \delta\mathbf{m} - is'' \mp R\,. \tag{27}$$

Here the notations are introduced

$$R = \sqrt{(\mathbf{p}\cdot\delta\mathbf{m} - ip'')^2 + (\mathbf{q}\cdot\delta\mathbf{m} - iq'')^2}\,; \tag{28}$$

$$\left.\begin{matrix}\mathbf{s}_0\\ \mathbf{p}\end{matrix}\right\} = \frac{1}{2\rho v_0}(\mathbf{A}_{01}\hat{c}\mathbf{A}_{01} \pm \mathbf{A}_{02}\hat{c}\mathbf{A}_{02})\mathbf{m}_0\,, \qquad \mathbf{q} = \frac{1}{2\rho v_0}(\mathbf{A}_{01}\hat{c}\mathbf{A}_{02} + \mathbf{A}_{02}\hat{c}\mathbf{A}_{01})\mathbf{m}_0\,; \tag{29}$$

$$\left.\begin{matrix}s''\\ p''\end{matrix}\right\} = \frac{Q''_{11} \pm Q''_{22}}{4\rho v_0}, \qquad q'' = \frac{Q''_{12}}{2\rho v_0}; \tag{30}$$

$$Q''_{ij} = \mathbf{A}_{0i}\cdot\hat{Q}''_0\mathbf{A}_{0j}\,. \tag{31}$$

The introduced vectors $\mathbf{s}_0$, $\mathbf{p}$ and $\mathbf{q}$ have the following projections on $\mathbf{m}_0$:

$$\mathbf{s}_0\cdot\mathbf{m}_0 = v_0\,, \qquad \mathbf{p}\cdot\mathbf{m}_0 = \mathbf{q}\cdot\mathbf{m}_0 = 0\,. \tag{32}$$

Note, that the vectors $\mathbf{s}_0$, $\mathbf{p}$ and $\mathbf{q}$ were first introduced by Fedorov (1968) in his theory of internal conical refraction. Then the same vectors were used in the theory of acoustic axes (Alshits, Sarychev & Shuvalov, 1985). With (27), systems (24) are easily solved which allows us to find the polarization vectors $\mathbf{A}_{1,2}$ (23) (not normalized at this stage):

$$\mathbf{A}_{1,2} = -(\mathbf{q}\cdot\delta\mathbf{m} - iq'')\mathbf{A}_{01} + (\mathbf{p}\cdot\delta\mathbf{m} - ip'' \pm R)\mathbf{A}_{02}\,. \tag{33}$$

It is easily checked that $\mathbf{A}_1\cdot\mathbf{A}_2 = 0$, i.e. the orthogonality property, eqn. (8), is fulfilled. Actually, eqns. (27) and (33) contain all necessary information for our further analysis. However, in the next section we shall have to make preliminary "step aside".

4. On the acoustic axes along directions of high symmetry

Note, that the above formalism linear in small parameters does not work for the case of tangent acoustic axes along which **p** = **q** = 0 (Alshits, Sarychev & Shuvalov, 1985) and one should keep the higher order terms in all expansions. The above criterion for a tangent degeneracy can be satisfied either because of an accidental vanishing of some combinations of material parameters (i.e. in model crystals) or due to a high symmetry of the direction $\mathbf{m}_0$. That is why tangent degeneracies are known in real crystals only along 4- and ∞-fold symmetry axes. In the first case the both Poincarè indices $n = \pm 1$ (Fig. 2) are possible, in the

latter case only the index n =+1 can occur (Alshits, Sarychev & Shuvalov, 1985). We already mentioned that model media are beyond our interest in this paper. As to "symmetrical" tangent acoustic axes, their reaction to "switching on" the damping is predictable without any calculations. The answer is rather natural: existing due to a symmetry which is not disturbed by the attenuation, they keep their directions and linear polarizations of the elastic waves propagating along them also retain, though the phase speeds v_a of these waves certainly take small imaginary components.

Indeed, the tensors $\hat{c}$ and $\hat{\eta}$ have completely the same symmetrical structure. It is well known, that along the direction $\mathbf{m}_0$ of the symmetry axis ∞ or *4* the tensor $\hat{Q}_0 = \mathbf{m}_0\hat{c}\mathbf{m}_0$ has eigenvectors $\mathbf{A}_{01}$,$\mathbf{A}_{02}$ and $\mathbf{A}_{03}$ coinciding with the basis vectors of the crystallographic coordinate system. Clearly, the tensor $\hat{Q}_0'' = \omega\mathbf{m}_0\hat{\eta}\mathbf{m}_0$ (20) must have the same eigenvectors. Hence, the combined complex Christoffel tensor $\hat{Q}' - i\hat{Q}'' = \hat{Q}_0 - i\hat{Q}_0''$ along the direction $\mathbf{m}_0$ admits purely real polarizations of three isonormal eigenwaves: one longitudinal ($\mathbf{A}_{03}$ parallel to *z*) and two transverse ($\mathbf{A}_{01}$ parallel to *x* and $\mathbf{A}_{02}$ parallel to *y*). It is easy to check that the degeneracy along $\mathbf{m}_0$ also retains. In accordance with eqn. (7)

$$\begin{aligned} \rho v_1^2 &= c_{1331} - i\omega\eta_{1331} = c_{55} - i\omega\eta_{55}, \\ \rho v_2^2 &= c_{2332} - i\omega\eta_{2332} = c_{44} - i\omega\eta_{44}, \\ \rho v_3^2 &= c_{3333} - i\omega\eta_{3333} = c_{33} - i\omega\eta_{33}. \end{aligned} \tag{34}$$

But the symmetry axes ∞ or *4* present only in tetragonal, cubic and hexagonal crystals where

$$c_{44} = c_{55}, \qquad \eta_{44} = \eta_{55} \tag{35}$$

and therefore $v_1 = v_2$. Accordingly, the degenerate tensor $\hat{Q}_0 - i\hat{Q}_0''$ has the spectral representation

$$\hat{Q}_0 - i\hat{Q}_0'' = [c_{44} - c_{33} - i\omega(\eta_{44} - \eta_{33})]\hat{I} + (c_{33} - i\,\omega\eta_{33})\mathbf{A}_{03} \otimes \mathbf{A}_{03} \tag{36}$$

where $\hat{I}$ denotes the unit tensor and the symbol $\otimes$ means a dyadic product. So, one can see, that any linear combination $a\mathbf{A}_{01} + \beta\mathbf{A}_{02}$ is also an eigenvector of $\hat{Q}_0 - i\hat{Q}_0''$ and any transverse wave may propagate along $\mathbf{m}_0$ (Fig.3). Note in addition, that in the considered situation the nominator $\mathbf{A}_{01} \cdot \hat{Q}''\mathbf{A}_{02}$ of the singular term in eqn. (15) vanishes together with η_{45}. This explains why our qualitative expectations of increasing imaginary components $\mathbf{A}_{1,2}''$ close to $\mathbf{m}_0$ have not been realized.

The same arguments are equally applicable for the directions of *3*-fold symmetry axes along which the conical acoustic axes necessarily occur (Alshits, Sarychev & Shuvalov, 1985) being characterized by the polarization singularity with the Poincarè index $n = -1/2$ (Fig. 2). However in this case $\mathbf{p} \neq \mathbf{q} \neq 0$ and the formalism developed in the previous section does work and may be used for the demonstration of the validity of the above considerations. For example, in the case of the *3*-fold symmetry axis in trigonal crystal one has: $p'' \propto \eta_{1331} - \eta_{2332} = \eta_{55} - \eta_{44} = 0$ and $q'' \propto \eta_{1332} = \eta_{54} = 0$ but $s'' \propto \eta_{1331} + \eta_{2332} = 2\eta_{44} \neq 0$. As a result, the phase speed perturbations $\delta v_{1,2}$, eqn. (27), have the equal imaginary components and the difference between δv_1 and δv_2 remains purely real and vanishes at $\delta\mathbf{m} \to 0$. Thus,

again there is neither a split nor a shift of the degeneracy. And in accordance with eqn. (33) the degenerate polarization fields $\mathbf{A}_{1,2}$ in the neighbourhood of the acoustic axis in the leading approximation remain linear, i.e. their imaginary components are small and vanish at $\delta\mathbf{m} \to 0$.

But such a trivial situation occurs only along the symmetry axes ∞, *4* and *3*. As we shall see, any other point of degeneracy, even in a symmetry plane, manifests instability with respect to attenuation and singular behaviour of basic wave parameters close to new acoustic axes.

Let us consider the other "symmetric" case known in real crystals: the line of degeneracy which occurs in some transversely isotropic media. According to (Alshits, Sarychev & Shuvalov, 1985), along such line: $\mathbf{p}\times\mathbf{q} = 0$ i.e. the vectors $\mathbf{p}$ and $\mathbf{q}$ must be parallel or one of them should vanish (let $\mathbf{q} = \gamma\mathbf{p}$ say). Note that at $\mathbf{p}\times\mathbf{q} = 0$ the point degeneracy is also possible (in model crystals, of course). In this case for its description one should keep in expansions the terms of the higher order. But for a line degeneracy the leading approximation used above is completely sufficient and eqns. (27) and (33) may be applied for an analysis. The condition of the degeneracy $\delta v_1 = \delta v_2$ is equivalent to the requirement of the vanishing square root in (27) which brings us to the following system

$$(\mathbf{p}\cdot\delta\mathbf{m})^2 + (\mathbf{q}\cdot\delta\mathbf{m})^2 - p''^2 - q''^2 = 0\,, \tag{37}$$

$$p''(\mathbf{p}\cdot\delta\mathbf{m}) + q''(q\cdot\delta\mathbf{m}) = 0\,. \tag{38}$$

At $\mathbf{q} = \gamma\mathbf{p}$ this system becomes clearly contradictive,

$$\mathbf{p}\cdot\delta\mathbf{m} = \sqrt{(p''^2 + q''^2)/(1+\gamma^2)}\,,$$

$$\mathbf{p}\cdot\delta\mathbf{m} = 0\,,$$

and has no solutions unless the both parameters p'' and q'' simultaneously vanish which does not occur in hexagonal crystals. Thus the line degeneracy $\mathbf{p}\cdot\delta\mathbf{m} = 0$ under the damping perturbation must completely disappear which coincide with the corresponding conclusion in (Shuvalov & Chadwick, 1997). But looking at eqns. (27) and (33) one can say more. It follows from (27) that at $\mathbf{p}\cdot\delta\mathbf{m} = 0$ the perturbations $\delta v_{1,2}$ are purely imaginary. This means that real components of the phase speeds v_{01} and v_{02} coincide as before on the same line $\mathbf{p}\cdot\delta\mathbf{m} = 0$. However, the imaginary components $\delta v''_{1,2}$ are different on this line which eliminates the degeneracy. As regards to polarizations, the only peculiarity of the polarization field on the line $\mathbf{p}\cdot\delta\mathbf{m} = 0$ is the lack of even a symbolic ellipticity: by (33) it is purely linear.

5. Split of acoustic axes of general positions

At the switched off attenuation eqn. (27) transforms to the known equation (Alshits, Sarychev & Shuvalov, 1985) describing local geometry of sheets of the phase velocity surface *P*: $v_{1,2}(\mathbf{m}) = v_0 + \delta v_{1,2}(\mathbf{m}_0 + \delta\mathbf{m})$ in the vicinity of the degeneracy point $v_1(\mathbf{m}_0) = v_2(\mathbf{m}_0) = v_0$:

$$\delta v_{1,2} = \mathbf{s}_0\cdot\delta\mathbf{m} \mp \sqrt{(\mathbf{p}\cdot\delta\mathbf{m})^2 + (\mathbf{q}\cdot\delta\mathbf{m})^2}\,. \tag{39}$$

If the vectors **p** and **q** are neither vanishing nor parallel to each other, $\mathbf{p}\times\mathbf{q}\neq 0$, then eqn.(39) describes a conical contact of the sheets $v_{1,2}(\mathbf{m})$ and simultaneously of the sheets $1/v_{1,2}(\mathbf{m})$ of the slowness surface *S*. This is a conical degeneracy of a general type not related to symmetry of a crystal.

As we know, a "switching on" the attenuation causes a small imaginary addition to a phase speed of the wave: $v=v'-iv''$. As a result, apart from the wave surfaces *P* and *S* the new surface of attenuation, $v''(\mathbf{m})$, arises. And the real components of the phase speeds $v'_{1,2}(\mathbf{m})$ also manifest important changes providing a topological transformation of the wave surfaces *P* and *S*.

Let us return to eqns. (37), (38). At $\mathbf{p}\times\mathbf{q}\neq 0$ this system describes the split of conical acoustic axis due to a damping. The new positions of the degeneracies $\delta\mathbf{m}_1$ and $\delta\mathbf{m}_2$ are given by the intersection of the ellipse

$$\left(\frac{\delta\mathbf{m}\cdot\mathbf{p}}{r}\right)^2+\left(\frac{\delta\mathbf{m}\cdot\mathbf{q}}{r}\right)^2=1, \qquad r=\sqrt{p''^2+q''^2}, \tag{40}$$

with the straight line $\delta\mathbf{m}\cdot\mathbf{M}=0$ passing through the end of the vector $\mathbf{m}_0$ perpendicularly to the vector (Fig. 4)

$$\mathbf{M}=p''\mathbf{p}+q''\mathbf{q}=r(\mathbf{p}\sin a+\mathbf{q}\cos a), \tag{41}$$

where the angle a is introduced by the expressions

$$\sin a=p''/r, \qquad \cos a=q''/r. \tag{41a}$$

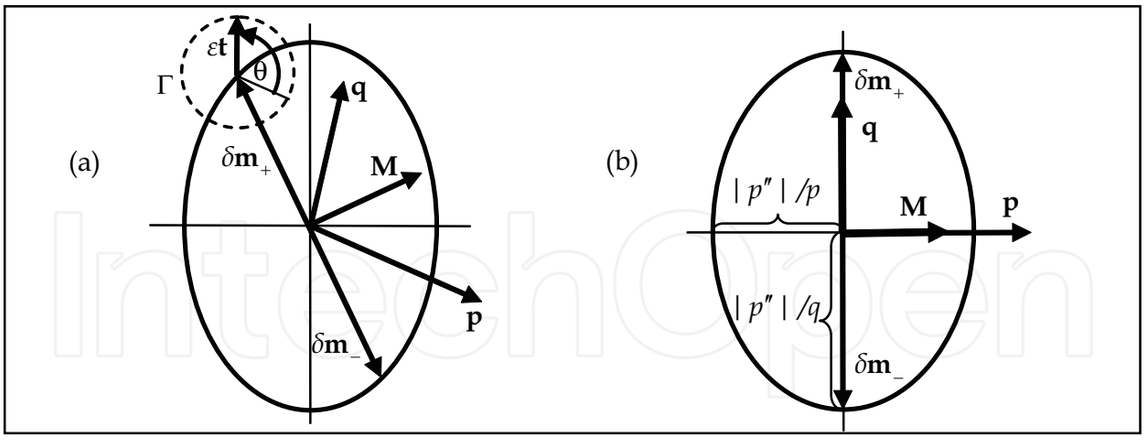

Fig. 4. Schematic plot of the ellipse, eqn. (40), in the general case (a), and for the case of the conical acoustic axis $\mathbf{m}_0$ splitting from the symmetry plane of a crystal (b)

In accordance with eqn. (32) the both vectors **p** and **q** are orthogonal to $\mathbf{m}_0$. Therefore the ellipse (40) (Fig.4) belongs to the plane tangent to the unit sphere $\mathbf{m}\cdot\mathbf{m}=1$ at the point $\mathbf{m}=\mathbf{m}_0$ which indicates the center of the ellipse. Thus, "switching on" the damping causes the split of the conical axis $\mathbf{m}_0$ into the two singular axes directed along the wave normals $\mathbf{m}_\pm=\mathbf{m}_0+\delta\mathbf{m}_\pm$ where

$$\delta\mathbf{m}_{\pm} = \pm\frac{\mathbf{m}_0\times(p''\mathbf{p}+q''\mathbf{q})}{\mathbf{m}_0\cdot(\mathbf{p}\times\mathbf{q})}\,. \tag{42}$$

Note that the projections of $\delta\mathbf{m}_{\pm}$ (42) on $\mathbf{p}$ and $\mathbf{q}$ vectors look rather simple

$$\delta\mathbf{m}_{\pm}\cdot\mathbf{p} = \mp q'', \quad \delta\mathbf{m}_{\pm}\cdot\mathbf{q} = \pm p''\,. \tag{43}$$

Let us consider the example of splitting of a conical axis belonging to the symmetry plane S of the crystal. It is evident that in this case the polarization vector $\mathbf{A}_{03}$ also belongs to the plane S. The other vectors of our basis may be chosen so that, say, the vector $\mathbf{A}_{01}$ is directed along the normal to the plane S, and the vector $\mathbf{A}_{02}$ belongs to the same plane S together with the vectors $\mathbf{m}_0$ and $\mathbf{A}_{03}$ (Fig. 5a). It is easily checked that in the given case due to a crystal symmetry, which is not less than monoclinic, there must be

$$q'' = 0, \quad \mathbf{q}\ \|\mathbf{A}_{01}, \quad \mathbf{p}\ \|\mathbf{A}_{01}\times\mathbf{m}_0 \tag{44}$$

(Fig. 5b). By eqns. (43), (44), the split from the symmetry plane is determined by the vectors

$$\delta\mathbf{m}_{\pm} = \pm\frac{|p''|}{q}\mathbf{A}_{01}\,. \tag{45}$$

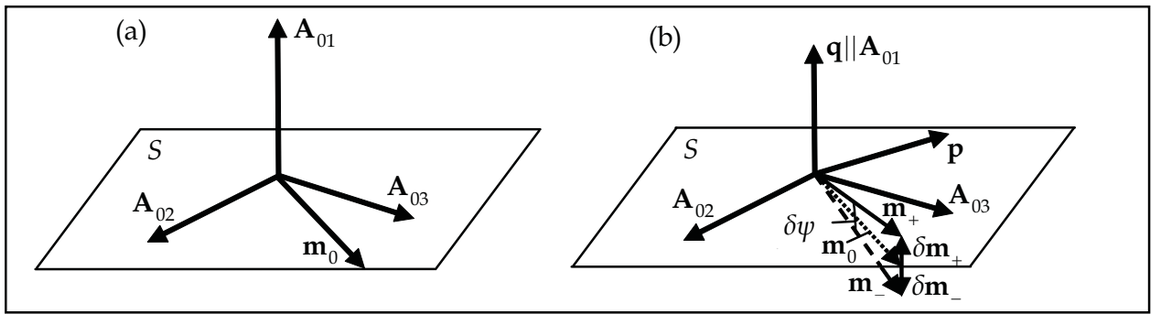

Fig. 5. Acoustic axis $\mathbf{m}_0$ in symmetry plane S (a), and its splitting due to the damping (b)

For the found mutual orthogonality of the vectors $\mathbf{p}$ and $\mathbf{q}$ ellipse (40) looks very symmetric (Fig. 4b). Thus, in the considered particular case the split of the acoustic axis occurs in the plane orthogonal to S and the angle $\delta\psi$ of splitting is proportional to the damping (Fig. 5b)

$$\delta\psi \approx 2\,|\,\delta m_{\pm}\,| = 2\,|\,p''\,|/q\,. \tag{46}$$

6. Local geometry of the velocity surfaces in the vicinity of split axes

Let us now return to eqns. (27), (28). We shall not divide eqn. (27) on the real and imaginary parts. It is more convenient to analyse this equation in its combined form. First of all, let us note that the expression under square root in eqn. (28) along the line $\delta\mathbf{m}\cdot\mathbf{M} = 0$ is purely real, being negative between the degeneracy points (i.e. inside the ellipse, eqn. (40) and Fig.4) and positive beyond them (i.e. outside the ellipse). But this means that on the part of this line which is inside of the ellipse, the square root is purely imaginary. Accordingly, on

this part of the line the real components of phase speed $v'_1(\mathbf{m})$ and $v'_2(\mathbf{m})$ must coincide which creates the lines of self-intersection of the wave surfaces $v'_{1,2}(\mathbf{m})$ and $1/v'_{1,2}(\mathbf{m})$. Quite similarly, we come to the conclusion that the corresponding sheets of the attenuation surface $v''_{1,2}(\mathbf{m})$ must intersect each other over the line $\delta\mathbf{m}\cdot\mathbf{M}=0$ outside the ellipse (40). Fig. 6 gives a schematic illustration of such self-intersection of the slowness surface.

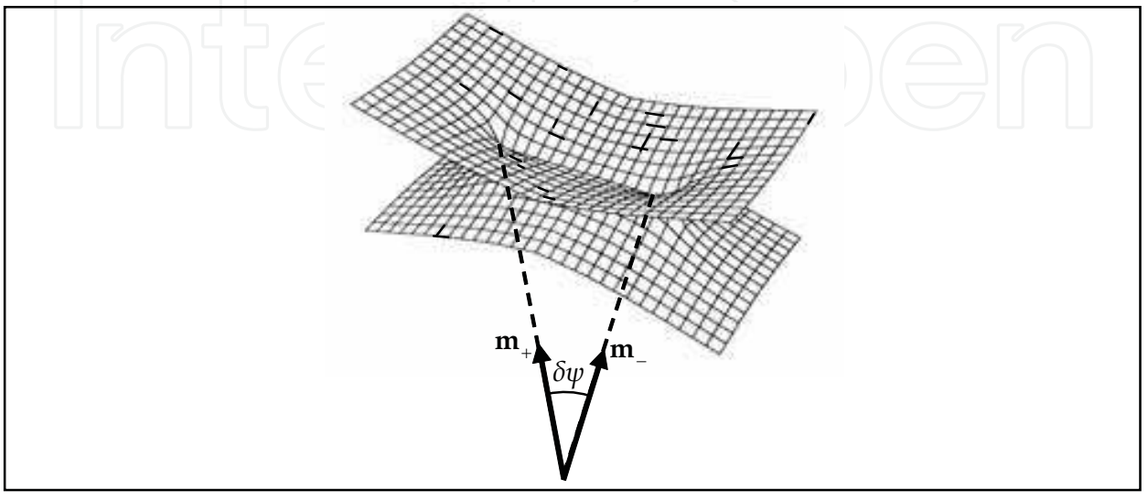

Fig. 6. Self-intersection of the slowness surface $1/v'_{1,2}(\mathbf{m})$ and split acoustic axes

Now let us study the above surfaces close to one of the new degeneracies, say, $\mathbf{m}_+ = \mathbf{m}_0 + \delta\mathbf{m}_+$. We are going to find the phase speeds of isonormal waves at the contour Γ (Fig. 4a): $\mathbf{m} = \mathbf{m}_+ + \delta\mathbf{m}_\varepsilon(\theta)$. The contour lies in the plane orthogonal to $\mathbf{m}_0$ and its radius is supposed to be small: $\varepsilon = |\delta\mathbf{m}_\varepsilon| << |\delta\mathbf{m}_+|$. Denote

$$\delta\mathbf{m}_\varepsilon(\theta) = \varepsilon\mathbf{t}(\theta), \tag{47}$$

where $\mathbf{t}$ is the unit vector making the angle θ with the vector $\mathbf{p}$:

$$\mathbf{t}(\theta) = [\mathbf{p}\cos\theta + (\mathbf{m}_0\times\mathbf{p})\sin\theta]/p. \tag{48}$$

Thus, by changing θ from 0 to 2π, the vector $\delta\mathbf{m}_\varepsilon$ (47) path-traces the contour Γ around the degeneracy point $\delta\mathbf{m}_+$ (Fig. 4a).
With (47), (48), eqn. (27) gives in the leading approximation over ε at the contour Γ:

$$\delta v'_{1,2}(\varepsilon,\theta) = v'_{1,2} - v'_{0+} = \mp\sqrt{\varepsilon}\,\mathrm{Re}[f(\theta)], \tag{49}$$

where

$$f(\theta) = \sqrt{2\mathbf{t}\cdot(\mathbf{N} - i\mathbf{M})}, \qquad \mathbf{N} = -q''\mathbf{p} + p''\mathbf{q}. \tag{50}$$

As is seen from (49), the dependence $\delta v'_{1,2}(\varepsilon)\propto\sqrt{\varepsilon}$ at $\varepsilon\to 0$ is characterized by an infinite derivative over ε in any section $\theta\neq\theta_0$, where the angle θ_0 relates to a transition of the vector $\delta\mathbf{m}_\varepsilon$ through the self-intersection line, $\mathrm{Re}[f(\theta_0)]=0$. This singularity of the function

$\delta v'_{1,2}(\varepsilon)$ at the end of the wedge of self-intersection corresponds to a sharpening tip of the slowness surface $1/v'_{1,2}(\mathbf{m})$ and to a plane fan of the normals to this surface at the contour Γ when $\varepsilon \to 0$ (Fig. 7).

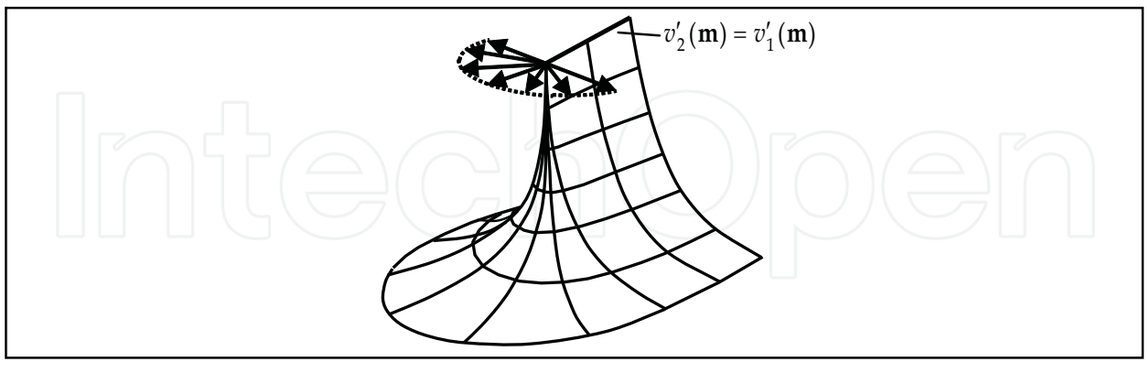

Fig. 7. The fragment of the internal degenerate sheet $1/v'_2(\mathbf{m})$ of the slowness surface close to the singular point at the end of the wedge of the self-intersection and the plane fan of normals to the surface at this point

7. Polarization field singularities around the split acoustic axes

At the same contour Γ (47) polarization vectors (33) up to normalizing factors are equal

$$\mathbf{A}_{1,2} = \mathbf{A}_{01} + i\left(1 \mp \frac{\sqrt{\varepsilon} f(\theta)}{q'' + ip''}\right)\mathbf{A}_{02}\,. \tag{51}$$

For the further analysis the function $f(\theta)$ here should be concretize to the form

$$f(\theta) = A\sqrt{\mathbf{p}\cdot\mathbf{q}\cos\theta + g\sin\theta - ip^2\cos\theta}\,, \tag{52}$$

where

$$A = \sqrt{2(p'' - iq'')/p}\,, \qquad g = \mathbf{m}_0\cdot(\mathbf{p}\times\mathbf{q})\,. \tag{53}$$

It is easily checked, that at the rotation of unit vector **t**, (48), over the whole circuit, i.e. at varying θ from 0 to 2π, the function $f(\theta)$ (52), changes its sign. Indeed, the phase of the complex function

$$f(\theta)/A \equiv R(\theta)\exp[i\Psi(\theta)] \tag{54}$$

must be twice less than the phase of its square

$$R^2\exp(2i\Psi) = \mathbf{p}\cdot\mathbf{q}\cos\theta + g\sin\theta - ip^2\cos\theta\,. \tag{55}$$

On the other hand, one can find from (55) the following relations

$$\Psi(\theta) = -\frac{1}{2}\left(\mathrm{Arctg}\frac{p^2}{\mathbf{p}\cdot\mathbf{q} + g\,\mathrm{tg}\theta}\right), \qquad \frac{\partial\Psi}{\partial\theta} = \frac{gp^2\cos^2 2\Psi}{(\mathbf{p}\cdot\mathbf{q}\cos\theta + g\sin\theta)^2}\,. \tag{56}$$

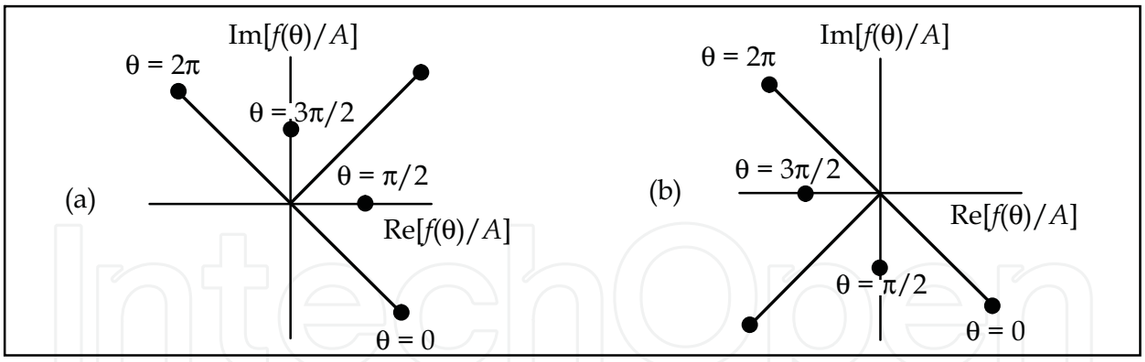

Fig. 8. The function $f(\theta)/A$ in the complex plane at $g > 0$ (a) and $g < 0$ (b)

This gives (see also Fig. 8)

$$\Psi(2\pi) - \Psi(0) = \pi \mathrm{sgn} g\,, \tag{57}$$

$$f(2\pi) = -f(0)\,. \tag{58}$$

Thus, after the whole turn over the contour Γ around the degeneracy point at $\delta\mathbf{m}_+$ (Fig. 4a) one has the identical transformation of the polarization field (51) in itself in the form

$$\mathbf{A}_1(2\pi) = \mathbf{A}_2(0)\,, \quad \mathbf{A}_2(2\pi) = \mathbf{A}_1(0)\,. \tag{59}$$

In other words, each of two orthogonal polarization ellipses rotates exactly on $\pi/2$ being transformed into the polarization of the isonormal wave (Fig. 9). And simultaneously the complex velocities $v_{1,2} = v'_{1,2} - iv''_{1,2}$ also are interchanging with their counterparts (Fig. 10).

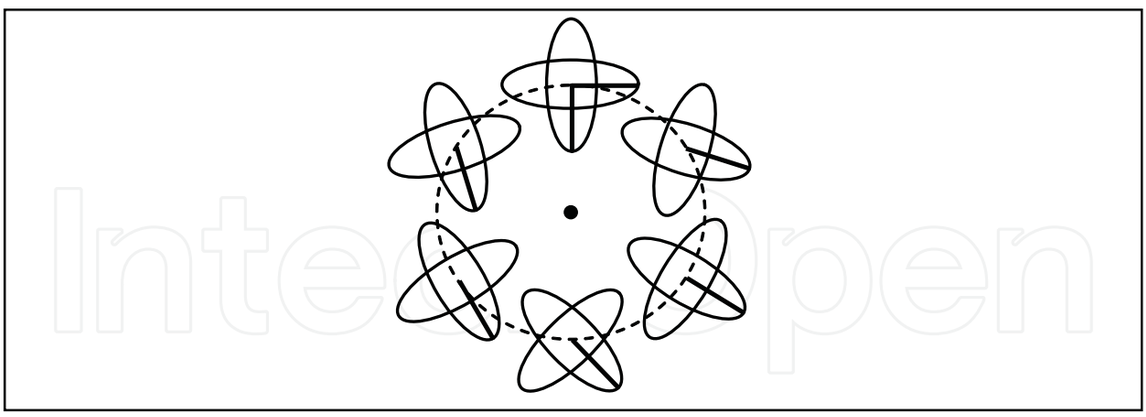

Fig. 9. The rotation of the polarization ellipses $\mathbf{A}_{1,2}$ in the degeneracy plane D when the wave normal $\mathbf{m}$ is scanning the contour Γ. The case $g > 0$ is shown when $n = ¼$.

The found singularity of the polarization field at the degeneracy point $\mathbf{m}_+$ (Fig. 9) may be characterized by the Poincarè index defined as the value of the total polarization rotation (in the 2π units) at a complete path-tracing over the contour Γ around this point. The found turn of the polarization ellipses is equal $\pi/2$, and the direction of the rotation, by eqn. (57), is determined by the sign of the parameter g (53). Hence, one has (Alshits & Lyubimov, 1998)

$$n = \frac{1}{4}\mathrm{sgn}[\mathbf{m}_0 \cdot (\mathbf{p} \times \mathbf{q})] \tag{60}$$

It is easily verified that the same relation is valid for the second degeneracy point $\mathbf{m}_-$.

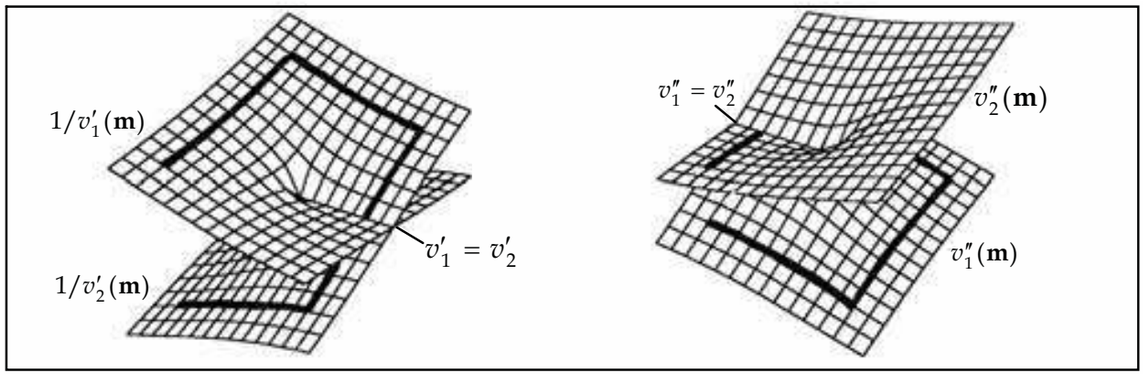

Fig. 10. The surfaces $1/v'_{1,2}(\mathbf{m})$ and $v''_{1,2}(\mathbf{m})$ in the vicinity of the acoustic axis $\mathbf{m}_+$. The transition between the sheets of the surfaces when $\mathbf{m}$ is scanning the contour around $\mathbf{m}_+$

Thus the physical equivalence of two pictures at $\theta = 0$ and $\theta = 2\pi$ is realized not by a coincidence of the wave characteristic inside each of the branches, as it occurs at zero damping, but by the identity of their superpositions. This becomes topologically possible due to such a new feature of the slowness surfaces as their self-intersections (Fig. 10). In the absence of damping, when the degenerate wave sheets locally have the only contact point, one of the branches along any direction is always "faster" than the other. And the related polarization cross, contained of isonormal linear non-directed vectors, has non-equivalent "differently coloured" crosspieces. Hence for a coincidence of such cross with itself it is required its turn on the minimum angle π, instead of $\pi/2$, as in the above case (Figs. 9, 10). The turn on $\pi/2$ is sufficient only when the change of "colours" of crosspieces occurs during the turn.

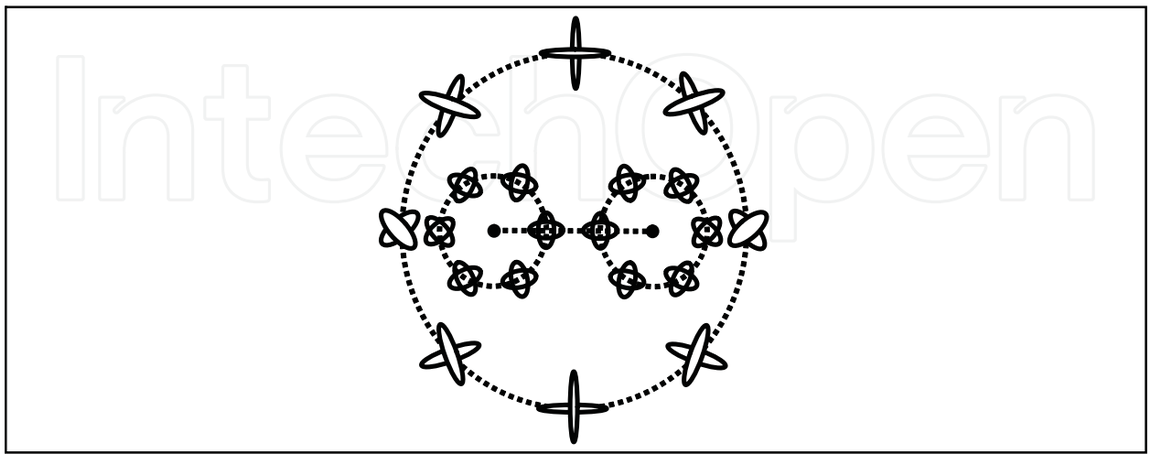

Fig. 11. The field of elliptic polarizations of degenerate branches in the vicinity of split axes of an absorptive crystal for $g < 0$. The Poincarè indices at small contours are $n = -1/4$, and the combined index at the external contour is $n = -1/2$

That is why (Alshits, Sarychev & Shuvalov, 1985) in the absence of the damping a conical axis along $\mathbf{m}_0$ is characterized by the Poincarè index $n = (1/2)\mathrm{sgn}g$. This is the minimal index for a real polarization field. Its splitting into the two singularities (60) due to "switching on" attenuation satisfies the index conservation law. On the other hand, the same combined index $\pm 1/2$ arises at the path-tracing of the both points $\mathbf{m}_\pm$ (Fig. 11).

8. Conical refraction in absorptive crystals

Internal conical refraction of elastic waves in crystals is a good example of a non-trivial role of anisotropy, which may create new phenomena principally impossible in isotropic media. The energy flux $\mathbf{P}$ of the wave in crystal is, as a rule, non-parallel to its direction $\mathbf{m}$ of propagation. For any wave normal $\mathbf{m}$ the direction of the Poynting vector $\mathbf{P}$ is determined by the orientation of the normal $\mathbf{n}$ to the slowness surface. At the choice of the wave normal along a conical acoustic axis each polarization vector in the degeneracy plane D (Fig. 3) relates to the definite Poynting vector, i.e. to the definite normal to a cone. Rotation of the polarization in the plane D (e.g. in a circularly polarized wave) should create a precession of the energy flux $\mathbf{P}$.

This phenomenon called the internal conical refraction was theoretically predicted and experimentally discovered by De Klerk & Musgrave (1955). They found a circular cone of refraction along the 3-fold symmetry axis in the cubic crystal Ni. Later on the more general cases of the refraction cones of elliptic section were theoretically studied (Barry & Musgrave, 1979; Khatkecich, 1962b; Musgrave, 1957) and experimentally found (Aleksandrov & Ryzhova, 1964). The complete theory of this phenomenon is presented in the monographs (Fedorov, 1968; Sirotin & Shaskolskaya, 1983). Below we shall develop an extension of this theory for absorptive crystals following to the recent paper (Alshits & Lyubimov, 2011).

8.1 Conical refraction in the absence of attenuation

As we have seen, in a crystal without damping along the acoustic axis $\mathbf{m}_0$, apart from the non-degenerate wave with the polarization vector $\mathbf{A}_{03}$, an infinite number of elastic waves may propagate with arbitrary polarization in the degeneracy plane D (Fig. 3). Thus in the basis $\{\mathbf{A}_{01}, \mathbf{A}_{02}\}$ belonging to the same plane, for any angle β the vector

$$\mathbf{A}(\beta) = \mathbf{A}_{01}\cos\beta + \mathbf{A}_{02}\sin\beta \tag{61}$$

determines polarization of the eigenwave propagating along $\mathbf{m}_0$ with the phase speed v_0. Certainly, the wave with a circular polarization $\mathbf{A} = \mathbf{A}_{01} + i\mathbf{A}_{02}$ can also propagate along the same direction.

Consider a monochromatic plane wave propagating along the acoustic axis $\mathbf{m}_0$ with the polarization $\mathbf{A}$ and the phase speed v_0:

$$\mathbf{u}(\mathbf{r}, t) = C\mathbf{A}\exp(i\Phi_0), \qquad \Phi_0 = k(\mathbf{m}_0 \cdot \mathbf{r} - v_0 t). \tag{62}$$

The Poynting vector of such wave is equal (Fedorov, 1968)

$$\mathbf{P} = (\mathrm{Re}\dot{\mathbf{u}})\hat{c}(\mathrm{Re}\dot{\mathbf{u}})\mathbf{m}_0 / v_0. \tag{63}$$

For linear and circular polarizations one has, respectively,

$$\mathrm{Re}\mathbf{u}_{\mathrm{lin}} = C\mathbf{A}(\beta)\cos\Phi_0\,, \tag{64}$$

$$\mathrm{Re}\mathbf{u}_{\mathrm{cir}} = C[\mathbf{A}_{01}\cos\Phi_0 - \mathbf{A}_{02}\sin\Phi_0]\,. \tag{65}$$

In these two cases the Poynting vectors are given by different expressions:

$$\mathbf{P}_{\mathrm{lin}} = C^2\rho\omega^2(\mathbf{s}_0 + \mathbf{p}\cos 2\beta + \mathbf{q}\sin 2\beta)\sin^2\Phi_0\,, \tag{66}$$

$$\mathbf{P}_{\mathrm{cir}} = C^2\rho\omega^2(\mathbf{s}_0 - \mathbf{p}\cos 2\Phi_0 + \mathbf{q}\sin 2\Phi_0)\,. \tag{67}$$

Quite similarly one finds the elastic energy densities $W = \rho(\mathrm{Re}\dot{\mathbf{u}})^2$:

$$W_{\mathrm{lin}} = C^2\rho\omega^2\sin^2\Phi_0\,, \qquad W_{\mathrm{cir}} = C^2\rho\omega^2\,. \tag{68}$$

With eqns. (66)-(68), the ray velocities of the considered waves are equal

$$\mathbf{s}_{\mathrm{lin}} = \mathbf{P}_{\mathrm{lin}}/W_{\mathrm{lin}} = \mathbf{s}_0 + \mathbf{p}\cos 2\beta + \mathbf{q}\sin 2\beta\,, \tag{69}$$

$$\mathbf{s}_{\mathrm{cir}} = \mathbf{P}_{\mathrm{cir}}/W_{\mathrm{cir}} = \mathbf{s}_0 - \mathbf{p}\cos 2\Phi_0 + \mathbf{q}\sin 2\Phi_0\,. \tag{70}$$

During the period of the circularly polarized wave at a complete turn of the polarization vector in the degeneracy plane D, the ray velocity vector $\mathbf{s}_{\mathrm{cir}}$ (70) twice circumscribes a cone (Fig. 12). At that the end of the vector $\mathbf{s}_{\mathrm{cir}}$ twice path-traces the ellipse

$$\Delta\mathbf{s} = \mathbf{s} - \mathbf{s}_0 = -\mathbf{p}\cos 2\Phi_0 + \mathbf{q}\sin 2\Phi_0\,. \tag{71}$$

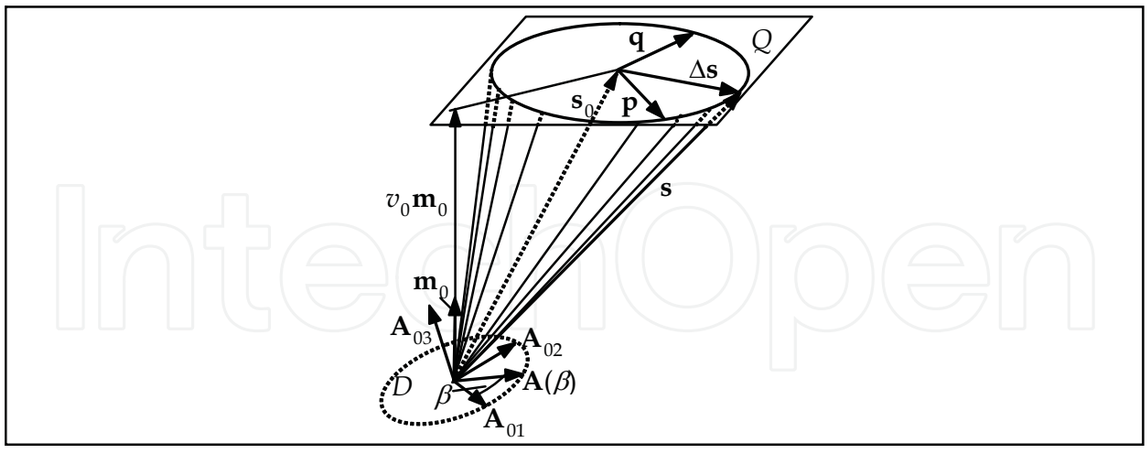

Fig. 12. The cone of the internal conical refraction

In view of (32), the plane Q of the ellipse is orthogonal to $\mathbf{m}_0$, and the directions of path-tracing of the vectors $\Delta\mathbf{s}$ and $\mathrm{Re}\mathbf{u}_{\mathrm{cir}}$ are the same when $g > 0$ and opposite when $g < 0$.
For a linearly polarized wave the same refraction cone is described by the vector $\mathbf{s}_{\mathrm{lin}}$ (69) when the angle β changes within the interval $0 \le \beta \le 2\pi$ (Fig. 12). This particular scheme was realized in the first experiments of De Klerk & Musgrave (1955).

8.2 The polarization ellipses at the ridge of the wedge of self-intersection

Consider now the wave characteristics of an absorptive crystal at the ridge of the wedge of self-intersection of the slowness surface. For a description of the set of wave normals related to the ridge between the two degeneracy points at the slowness surface let us introduce the vector $\delta\mathbf{m}_\xi = \delta\mathbf{m}_+ \sin\xi$. At changing ξ from $-\pi/2$ to $+\pi/2$ the vector $\delta\mathbf{m}_\xi$ moves through all the ridge from one degeneracy ($\delta\mathbf{m}_-$) to another one ($\delta\mathbf{m}_+$). Substitution $\delta\mathbf{m} = \delta\mathbf{m}_\xi$ into (33) gives the polarization vectors at any point of the line of self-intersection. Making use of relations (43) one obtains

$$\mathbf{A}_{1,2} = \frac{(\sin a \sin\xi - i\cos a)\mathbf{A}_{01} + [\cos a \sin\xi + i(\sin a \mp \cos\xi)]\mathbf{A}_{02}}{\sqrt{2(1 \mp \sin a \cos\xi)}}, \tag{72}$$

where the normalizing (9) is fulfilled and notations (41a) are used.

We remind that at the ridge of the wedge the real components of the phase speeds $v_{1,2}$ coincide: $v'_1 = v'_2 = v'_\xi$. The imaginary components $v''_{1,2}$ coincide only at the end points of the ridge, $\xi = \pm\pi/2$. In view of (6), the real components of the displacement vectors $\mathbf{u}_{1,2}$ take the form

$$\mathrm{Re}\mathbf{u}_{1,2}(\mathbf{r},\ t) = C_{1,2}\exp(-k''_{1,2}\mathbf{m}_\xi \cdot \mathbf{r})\mathrm{Re}[\mathbf{A}_{1,2}\exp(i\Phi_\xi)] \equiv C_{1,2}\exp(-k''_{1,2}\mathbf{m}_\xi \cdot \mathbf{r})\mathbf{U}_{1,2}\,. \tag{73}$$

We introduced here the wave normal $\mathbf{m}_\xi$ and the real phase Φ_ξ at the ridge,

$$\mathbf{m}_\xi = \mathbf{m}_0 + \delta\mathbf{m}_\xi\,, \qquad \Phi_\xi = k'_\xi \mathbf{m}_\xi \cdot \mathbf{r} - \omega t\,, \tag{74}$$

and the dimensionless displacement vectors

$$\mathbf{U}_{1,2} = \mathrm{Re}[\mathbf{A}_{1,2}\exp(i\Phi_\xi)]\,. \tag{75}$$

It is essential that in eqn. (73) a trivial damping of the wave $\propto \exp(-k''_{1,2}\mathbf{m}_\xi \cdot \mathbf{r})$ is separated from the vectors $\mathbf{U}_{1,2}$ describing much more important for us effects of attenuation.

In the considered stationary problem a choice of the time origin is certainly unessential and may be different for isonormal waves, independent from each other. Hence, the vectors $\mathbf{U}_{1,2}$ as well as the polarization vectors $\mathbf{A}_{1,2}$ are defined to the sign. Below this sign will be chosen so that our expression would be more compact.

Note, that at scanning the ridge by the wave normal $\mathbf{m}_\xi$, the elliptic polarization determined by eqns. (72), (75) is sharply changing. It is easily checked that this ellipticity provides rotations of the vectors $\mathbf{U}_{1,2}$ along the same directions corresponding to the right-hand screw along the propagation, until $\sin\xi > 0$, and to the left-hand screw, when $\sin\xi < 0$. At the ridge ends ($\xi = \pm\pi/2$) where the degeneracies occur, the isonormal waves, naturally, coincide: $\mathbf{U}_1 = \mathbf{U}_2 \equiv \mathbf{U}_0$. In both cases the polarization is circular however with different rotation "signs":

$$\begin{aligned} \mathbf{U}_0\big|_{\xi=\pi/2} &= \frac{1}{\sqrt{2}}(\mathbf{A}_{01}\cos\Phi_\xi - \mathbf{A}_{02}\sin\Phi_\xi), \\ \mathbf{U}_0\big|_{\xi=-\pi/2} &= \frac{1}{\sqrt{2}}(\mathbf{A}_{01}\cos\Phi_\xi + \mathbf{A}_{02}\sin\Phi_\xi). \end{aligned} \tag{76}$$

Here the angle α is excluded from the arguments by the choice of the time origin.
In any other points of the ridge the polarization ellipses of isonormal waves are different. In the middle point $\xi = 0$ the isonormal waves have linear polarizations orthogonal to each other:

$$\begin{aligned}\mathbf{U}_1\big|_{\xi=0} &= \left\{\mathbf{A}_{01}\cos\left(\frac{\pi}{4}-\frac{a}{2}\right)+\mathbf{A}_{02}\sin\left(\frac{\pi}{4}-\frac{a}{2}\right)\right\}\sin\Phi_0,\\ \mathbf{U}_2\big|_{\xi=0} &= \left\{\mathbf{A}_{01}\sin\left(\frac{\pi}{4}-\frac{a}{2}\right)-\mathbf{A}_{02}\cos\left(\frac{\pi}{4}-\frac{a}{2}\right)\right\}\sin\Phi_0.\end{aligned} \tag{77}$$

One can show that linear polarization retain on a whole line passing through the middle of the ridge ($\xi = 0$) perpendicular to it (at the unit sphere $\mathbf{m}^2 = 1$ this line passes through point $\mathbf{m}_0$ with local orientation along vector $\mathbf{M}$).
Expressions for the polarization ellipses of isonormal waves at the ridge are remarkably simplified in the considered above particular case related to the unperturbed acoustic axis $\mathbf{m}_0$ situated in the symmetry plane of the crystal. In this case $q'' = 0$. Supposing for definiteness that $p'' > 0$, one can put $a = \pi/2$. Then, instead of (72), the polarization vectors of the isonormal waves are equal

$$\begin{aligned}\mathbf{A}_1 &= \mathbf{A}_{01}\cos(\xi/2)+i\mathbf{A}_{02}\sin(\xi/2),\\ \mathbf{A}_2 &= \mathbf{A}_{01}\sin(\xi/2)+i\mathbf{A}_{02}\cos(\xi/2).\end{aligned} \tag{78}$$

And the rotation of the displacement vectors $\mathbf{U}_{1,2}$ (75) over the ellipses is now described by

$$\begin{aligned}\mathbf{U}_1 &= \mathbf{A}_{01}\cos(\xi/2)\cos\Phi-\mathbf{A}_{02}\sin(\xi/2)\sin\Phi\ ,\\ \mathbf{U}_2 &= \mathbf{A}_{01}\sin(\xi/2)\cos\Phi-\mathbf{A}_{02}\cos(\xi/2)\sin\Phi\ .\end{aligned} \tag{79}$$

These expressions represent ellipses in a parametric form. The lengths of the horizontal and vertical semi-axes of the first ellipse are equal $|\cos(\xi/2)|$ and $|\sin(\xi/2)|$, respectively. For the second ellipse the same length relate to the vertical and horizontal semi-axes. At the ridge ends $\xi = \pm\pi/2$ the above lengths of the semi-axes are equal to each other, and the polarization becomes circular. With a displacement of the "observation" point $\delta\mathbf{m}_\xi$ from the ridge ends to its middle the large semi-axes increase and the small semi-axes decrease to zero at $\xi = 0$.
Thus, both general expressions (76), (77) and the particular example (79) lead to the same picture of polarization distribution at the ridge of wedge of self-intersection. At passing along this line the isonormal waves, starting from a circular polarization of definite sign, monotonously decrease their ellipticity to zero in the middle of the ridge, where ellipses are transformed into non-directed vectors. At the second half of the ridge the ellipticity changes its sign and monotonously increases becoming circular at the other degeneracy point. Fig. 13 illustrates this behavior of polarization at the line of self-intersection of the slowness surface.
Consider now the kinematics of the motion of the displacement vectors of isonormal waves along the polarization ellipses. Express the radius-vectors $\mathbf{U}_a$ ($a = 1,2$) at the ellipse in polar coordinates (U_a, φ_a):

$$\mathbf{U}_a = U_a(\mathbf{A}_{01}\cos\varphi_a + \mathbf{A}_{02}\sin\varphi_a)\ . \tag{80}$$

Certainly, the lengths U_a of these radius-vectors at the ellipse depend on the azimuth φ_a. Comparing eqns. (72), (75) and (80), one has

$$U_{1,2}^2 = \frac{1}{2}\left(1 \pm \cos\xi \frac{(\sin a \mp \cos\xi)\cos 2\Phi_\xi + \sin\xi \cos a \sin 2\Phi_\xi}{1 \mp \sin a \cos\xi}\right), \tag{81}$$

$$\mathrm{tg}\,\varphi_{1,2} = \frac{\cos a \sin\xi - (\sin a \mp \cos\xi)\mathrm{tg}\,\Phi_\xi}{\sin a \sin\xi + \cos a\ \mathrm{tg}\,\Phi_\xi}. \tag{82}$$

Differentiating the latter expression with respect to time, it is easy to find the angular velocities $\dot{\varphi}_{1,2}$ of the radius-vectors $\mathbf{U}_{1,2}$ at their ellipses:

$$\dot{\varphi}_{1,2} = \frac{\omega \sin\xi}{2U_{1,2}^2}, \tag{83}$$

where we put $\dot{\Phi}_\xi = -\omega$. As is seen from (83), the angular velocities differently behave in time at different "observation" points at the ridge. Along the acoustic axes ($\xi = \pm\pi/2$), when the isonormal ellipses coincide into one circle (76), the denominator in (83) is equal to 1, and the circular motion has a constant angular velocity: $\dot{\varphi}_1 = \dot{\varphi}_2 = \pm\omega$. Here the upper and lower signs relate to different directions of the rotation at $\xi = \pm\pi/2$ (Fig. 13).

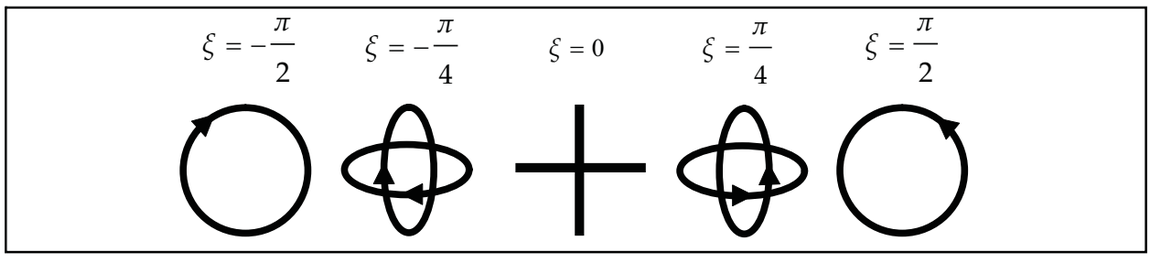

Fig. 13. Polarization distribution for isonormal waves at the line of self-intersection of the slowness surface

With decreasing $|\xi|$ a non-uniformity of the motion increases and at $|\xi| << 1$ acquires a singular character, when during the most part of the period the velocities $\dot{\varphi}_{1,2}$ are very small, and the azimuth angles $\varphi_{1,2}$ related to them are almost fixed. In this regime, the vectors $\mathbf{U}_{1,2}$ pass the most part of the ellipse in a short time with very high velocity. This is clearly seen from the analytical formulae related to the discussed above particular case of the acoustic axis splitting from the symmetry plane (Fig. 14):

$$\begin{aligned} \mathrm{tg}\,\varphi_1 &= -\mathrm{tg}(\xi/2)\mathrm{tg}\,\Phi_\xi, \\ \mathrm{tg}\,\varphi_2 &= -\mathrm{ctg}(\xi/2)\mathrm{tg}\,\Phi_\xi; \end{aligned} \tag{84}$$

$$\dot{\varphi}_{1,2} = \frac{\omega \sin\xi}{1 \pm \cos\xi \cos 2\Phi_\xi}. \tag{85}$$

Eqns. (81)-(85) and Fig. 14 show that the functions $\varphi_{1,2}(\Phi_\xi)$ and $\dot{\varphi}_{1,2}(\Phi_\xi)$ have the period twice less than the period of the wave. This means that the half-turn of the displacement vector over the polarization ellipse exhausts all its physically different orientations.

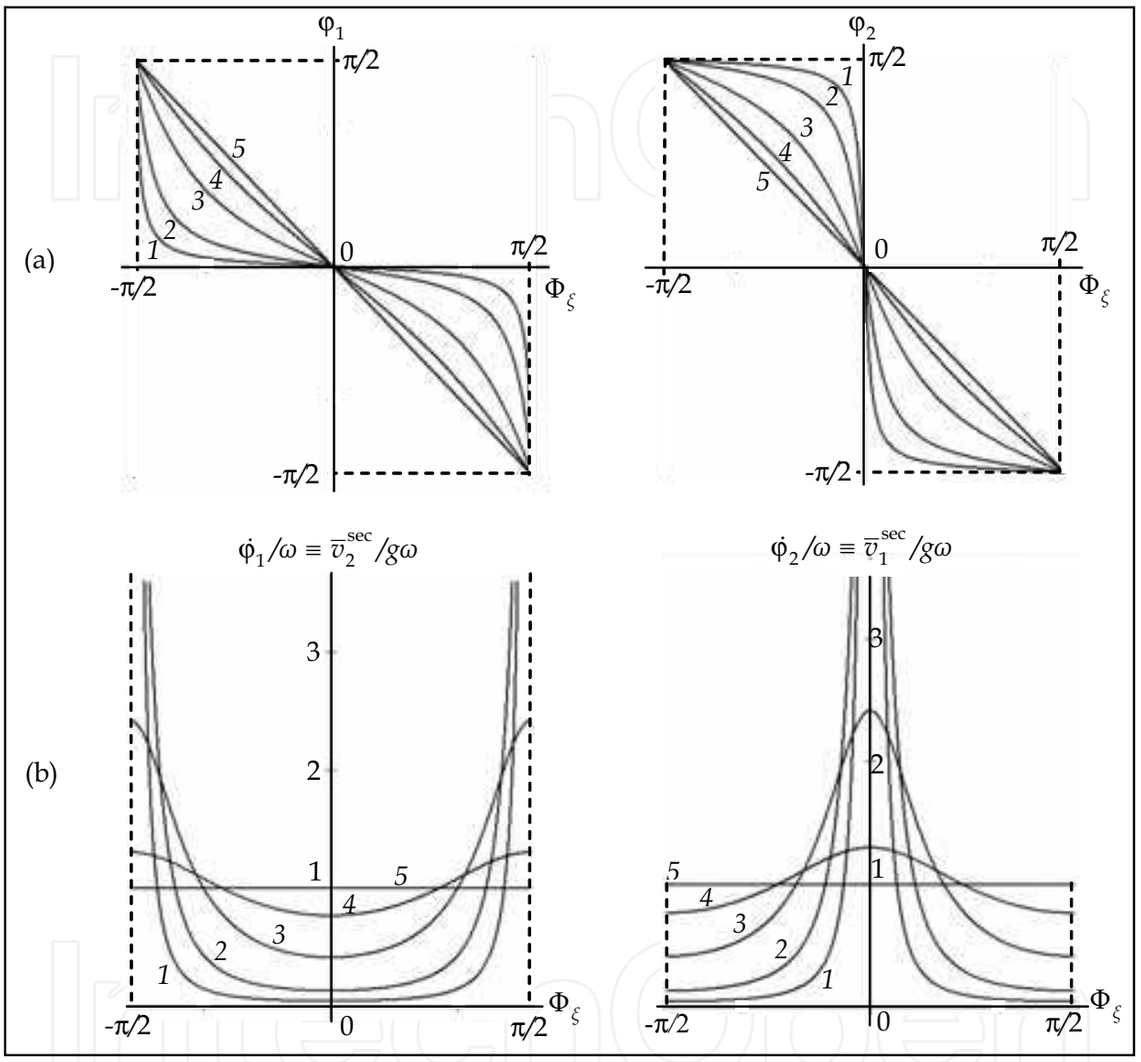

Fig. 14. Numerical plot of the azimuths $\varphi_{1,2}$ (84) (a) and the coinciding normalized speeds $\dot{\varphi}_{1,2}/\omega \equiv \bar{v}^{\text{sec}}_{2,1}/g\omega$ (85), (106) (b) versus the phase Φ_ξ for the series of "observation" points at the line of self-intersection of the slowness surface for a particular case of the acoustic axis splitting from the symmetry plane. *1* - $\xi = 5^\circ$, *2* - 15°, *3* - 45°, *4* - 75°, *5* - 90°

The other kinematic characteristics of the considered motion could be the so-called sectorial velocities defined as area circumscribed by a rotating vectors $\mathbf{U}_{1,2}$ per unit time:

$$v^{\text{sec}}_{1,2} = \frac{1}{2}U^2_{1,2}\dot{\varphi}_{1,2} = \frac{1}{4}\omega\sin\xi\,. \tag{86}$$

The found expression is valid for unrestricted anisotropy. It is identical for the both isonormal waves being independent of the time. However velocity (86) strongly depends on the position of the "observation" point at the line of self-intersection. In particular, it vanishes in the center of the ridge ($\xi = 0$), where the polarization becomes linear.

8.3 Universal refraction cone at the line of self-intersection and kinematics of ray velocity precession on this cone

Let us find the ray velocities of isonormal waves (73) at the ridge of self-intersection of the slowness surface $1/v'_{1,2}(\mathbf{m})$. Substituting (73) into (63) one obtains the energy flux

$$\mathbf{P}_{1,2} = |C_{1,2}\exp(-k''_{1,2}\mathbf{m}_\xi \mathbf{r})|^2\ \rho\omega^2[\mathbf{s}_0(F^2+G_\mp^2)-\mathbf{p}(G_\mp^2-F^2)+2\mathbf{q}FG_\mp], \tag{87}$$

where

$$F = \sin a\sin\xi\sin\Phi_\xi - \cos a\cos\Phi_\xi \tag{88}$$

$$G_\mp = \cos a\sin\xi\sin\Phi_\xi + (\sin a \mp \cos\xi)\cos\Phi_\xi . \tag{89}$$

The energy density in the isonormal waves in the same terms is equal

$$W_{1,2} = \rho(\mathrm{Re}\dot{\mathbf{u}}_{1,2})^2 = |C_{1,2}\exp(-k''_{1,2}\mathbf{m}_\xi \mathbf{r})|^2\ \rho\omega^2(F^2+G_\mp^2). \tag{90}$$

Accordingly, the ray velocities of these waves are given by

$$\mathbf{s}_{1,2} = \mathbf{P}_{1,2}/W_{1,2} = \mathbf{s}_0 - \mathbf{p}\cos 2\Theta_{1,2} + \mathbf{q}\sin 2\Theta_{1,2}, \tag{91}$$

where

$$\Theta_{1,2} = \Theta_{1,2}(a,\xi,\Phi_\xi), \qquad \mathrm{tg}\Theta_{1,2} = F/G_\mp . \tag{92}$$

Eqn. (91) is transformed from classic expression (70) for crystals without damping after the substitution in the latter $\Phi_0 \to \Theta_{1,2}$. This means that in an absorptive crystal at any point of the ridge of self-intersection the ends of the ray velocity vectors $\mathbf{s}_{1,2}$ move along the same trajectories, described by the universal ellipse

$$\Delta\mathbf{s}_{1,2} = -\mathbf{p}\cos 2\Theta_{1,2} + \mathbf{q}\sin 2\Theta_{1,2} . \tag{93}$$

The form of this ellipse is completely determined by the vectors **p** and **q**, and is independent of the parameters $\Theta_{1,2}$. In other words, it is insensitive neither to the phase Φ_ξ of the wave, nor to the angles α and ξ, related to parameters of damping and to a position of the "observation" point. The principal semi-axes of universal ellipse (93), coinciding with ellipse (71) for a non-attenuating medium, are equal

$$\lambda_{1,2} = \frac{1}{2}\left(\mathbf{p}^2+\mathbf{q}^2 \pm \sqrt{(\mathbf{p}^2+\mathbf{q}^2)^2 - 4(\mathbf{p}\times\mathbf{q})^2}\right). \tag{94}$$

Though the vectors **p** and **q** (29) do depend on a choice of the basis $\{\mathbf{A}_{01},\mathbf{A}_{02}\}$, one can easily check that their combinations $\mathbf{p}^2+\mathbf{q}^2$ and $\mathbf{p}\times\mathbf{q}$ determining semi-axes (94) are invariant with respect to orientation of this basis in the degeneracy plane *D* (Fig. 3).

With identical trajectories of the ray velocities precession at the whole ridge, the kinematics of their motion is very sensitive to the position ξ of the "observation" point. It may be shown that at the ridge ends $\xi = \pm\pi/2$ the values $\Theta_0(\pi/2)$ and $\Theta_0(-\pi/2)$ differ by only signs:

$$\Theta_0(\pm\pi/2) = \pm\Phi_\xi , \tag{95}$$

which gives, by (91),

$$\begin{aligned} \mathbf{s}(\pi/2) &= \mathbf{s}_0 - \mathbf{p}\cos 2\Phi_\xi + \mathbf{q}\sin 2\Phi_\xi , \\ \mathbf{s}(-\pi/2) &= \mathbf{s}_0 - \mathbf{p}\cos 2\Phi_\xi - \mathbf{q}\sin 2\Phi_\xi . \end{aligned} \tag{96}$$

This shows that the precession of the ray velocity vector along one of split acoustic axes is identical with the analogous process for a circularly polarized wave (70) propagating along the unsplit acoustic axis in the crystal without damping. Directions of rotation of the ray velocities $\mathbf{s}(\pm\pi/2)$ (96) have different signs. It is easily checked that at $g > 0$ they coincide with corresponding directions of circular polarization (76), and at $g < 0$ – are opposite to them.

In spite of the found identity of cones (70) and (96), there is an important difference between the related to them pictures of conical refraction. In the crystal without damping the ray velocities forming the refraction cone are directed along the appropriate normals to the slowness surface at the conical point of degeneracy. And the normals to the analogous surface in the vicinity of one of the split axes, as we have seen (Fig. 7), form a plane fan, which has nothing to do with a cone of ray velocities (96) (Fig. 12).

With passing of the "observation" point from the end of the ridge to its center, the motion of the ray velocity around universal cone (96) becomes less and less uniform. At the center point $\xi = 0$ the motion deceases at all: the isonormal vectors $\mathbf{s}_{1,2}$ are "frozen" at definite positions. Indeed, at $\xi = 0$ eqns. (88), (89) and (92) give the values $\Theta_{1,2}$ independent of time:

$$\Theta_{1,2} = \frac{a}{2} \pm \frac{\pi}{4} . \tag{97}$$

The corresponding fixed vectors of ray velocity are equal

$$\mathbf{s}_{1,2}(0) = \mathbf{s}_0 \pm (\mathbf{p}\sin a + \mathbf{q}\cos a) = \mathbf{s}_0 \pm \mathbf{M}/r . \tag{98}$$

As it would be expected, this result relates to expression (77) for a linear polarization of isonormal waves in the same way, as eqn. (69) to expression (64) from the refraction theory for crystals without damping. One can show that in this point ($\xi = 0$) of the ridge the two normals to the slowness surface are parallel not to vectors (98), but to their components belonging to the plane $\{\mathbf{m}_0, \mathbf{M}\}$ orthogonal to the ridge.

One should note that the fixed in time positions of the ray velocities (98) on ellipse (93) depend on the attenuation (the angle a, eqn. (41a)), whereas the universal ellipse does not "know" about a. This means that points (98), generally speaking, do not coincide with the ends of the principal semi-axes of the ellipse. Of course, in more symmetric situations the coincidence may occur, as it happens in the case of the splitting of the acoustic axis from a symmetry plane. What is more important that the vectors $\Delta\mathbf{s}_{1,2} = \mathbf{s}_{1,2}(0) - \mathbf{s}_0$, as it follows

from eqns. (98), (41) and Fig. 4, remain universally orthogonal to the ridge of the wedge at any changes of the angle a.

It is evident that at any small deviation of ξ from zero the fixed vectors (98) acquire some increments dependent on the phase Φ_ξ. This will renew a motion of the ray velocities $\mathbf{s}_{1,2}$ over the cone. However, if not to pass far from the middle point $\xi = 0$, the most part of the period the vectors $\mathbf{s}_{1,2}$ will retain orientations close to directions (98). And the time-averaged vectors $\bar{\mathbf{s}}_{1,2}$ in these points will be close to directions (98). This means that in the middle domain of the self-intersection line of the slowness surface, the refraction will have rather a wedge than a cone character.

In the considered above particular case of the acoustic axis splitting from the symmetry plane, one can put $a = \pi/2$ which remarkably simplifies expressions (88) and (89), and together with them also the formulae for angle parameters $\Theta_{1,2}$ (92):

$$\mathrm{tg}\Theta_1 = \mathrm{ctg}(\xi/2)\mathrm{tg}\Phi_\xi\,, \qquad \mathrm{tg}\Theta_2 = \mathrm{tg}(\xi/2)\mathrm{tg}\Phi_\xi\,. \tag{99}$$

The discussed problem of kinematics of the precession of ray velocities at the line of self-intersection of slowness surface may be quantitatively described. Introduce the polar coordinates ($S_{1,2}, \bar{\varphi}_{1,2}$) of the positions of the ends of the radius-vectors $\Delta\mathbf{s}_{1,2}$ at ellipses (93):

$$\Delta\mathbf{s}_{1,2} = S_{1,2}\left(\frac{\mathbf{p}}{p}\cos\bar{\varphi}_{1,2} + \frac{\mathbf{m}_0\times\mathbf{p}}{p}\sin\bar{\varphi}_{1,2}\right). \tag{100}$$

Comparing (100) with (93) one obtains

$$S_{1,2}^2 = (\mathbf{q}\sin\Theta_{1,2} - \mathbf{p}\cos\Theta_{1,2})^2 = \frac{q^2F^2 - 2\mathbf{p}\cdot\mathbf{q}G_\mp + p^2G_\mp^2}{F^2+G_\mp^2}\,, \tag{101}$$

$$\mathrm{ctg}\bar{\varphi}_{1,2} = (\mathbf{p}\cdot\mathbf{q} - p^2\mathrm{ctg}\Theta_{1,2})/g\,. \tag{102}$$

Differentiating the latter equation gives the angular velocities

$$\dot{\bar{\varphi}}_{1,2} = -\frac{g}{S_{1,2}^2}\dot{\Theta}_{1,2}\,. \tag{103}$$

Here the derivatives $\dot{\Theta}_{1,2}$ are found from (92):

$$\dot{\Theta}_{1,2} = \frac{\dot{F}G_\mp - F\dot{G}_\mp}{F^2+G_\mp^2} = -\frac{\omega\sin\xi}{U_{1,2}^2(\Phi_\xi+\pi/2)} = -2\dot{\varphi}_{1,2}(\Phi_\xi+\pi/2)\,, \tag{104}$$

where $U_{1,2}^2$ and $\dot{\varphi}_{1,2}$ are given by functions (81) and (83) shifted in phase: $\Phi_\xi \to \Phi_\xi + \pi/2$.

The sectorial velocities $\bar{v}_{1,2}^{sec}$ of the motion of the vectors $\Delta\mathbf{s}_{1,2}$ over universal ellipse (93) are found in analogy with eqn. (86):

$$\bar{v}_{1,2}^{sec} = \frac{1}{2}S_{1,2}^2\dot{\bar{\varphi}}_{1,2} = -\frac{1}{2}g\dot{\Theta}_{1,2} = g\dot{\varphi}_{1,2}(\Phi_\xi+\pi/2)\,. \tag{105}$$

Thus, this velocity differs from the angular velocity of the polarization, eqn. (83), only by the dimensional factor g and by the retardation $\pi/2$. Substituting into (105) the angular velocity $\dot{\varphi}_{1,2}$ (85) for the considered above symmetric example, one obtains the more compact form for the sectorial velocity:

$$\overline{v}_{1,2}^{sec}(\Phi_\xi) = \frac{g\omega\sin\xi}{1 \mp \cos\xi\cos 2\Phi_\xi} \equiv g\dot{\varphi}_{2,1}(\Phi_\xi)\,. \tag{106}$$

Here it is bearing in mind that the phase shift of the velocity $\dot{\varphi}_{1,2}$ in simplified variant (85) is equivalent to the transition at the counterpart branch: $\dot{\varphi}_{1,2}(\Phi_\xi + \pi/2) = \dot{\varphi}_{2,1}(\Phi_\xi)$. The found relation (106) allowed us to use in Fig. 14 the same curves for a characterization of both angular velocities of polarization and sectorial velocities of ray speeds. The shown dependencies adequately reflect the discussed above properties of the ray velocity precession at the line of self-intersection of the slowness surface. Angle velocities (103) behave in a similar way, especially in the region of small ξ. With closing to acoustic axes $\xi = \pm\pi/2$, variations of angular velocities in time are smoothing, but retain finite until $p \neq q$, in contrast to the velocities $\overline{v}_{1,2}^{sec}$, which tend to constant at these limits.

9. Conclusions

Thus, we have found that specific features of the influence of attenuation on the basic wave properties are associated with two main qualities of the damping: i) it does not disturb the symmetry of a crystal, and ii) formally, it provides an imaginary, i.e. non-hermitian, perturbation of the acoustic tensor. Due to the first quality there is almost no influence of the damping on the acoustic axes which exist due to symmetry of the crystal (tangent degeneracies along ∞ and *4*-fold symmetry axes and conical degeneracies along *3*-fold axes). On the other hand, the conical acoustic axes of any other orientations manifest instability with respect to an imaginary perturbation of the acoustic tensor. They split into pairs of degeneracies of new type (the so-called singular acoustic axes), which never occurs without damping. In the neighbourhood of split acoustic axes the polarization of elastic waves proves to be strongly elliptical becoming almost circular close to the degeneracy points. A rotation of the polarization ellipses around those points is described by the Poincarè index $n = \pm 1/4$. The slowness surface acquires lines of self-intersection connecting the split singular acoustic axes. Only the end points of these lines correspond to true degeneracies where the imaginary components of phase speeds of isonormal waves also coincide. The latter coincidence also occurs on the whole equi-damping lines at the attenuation surface. These self-intersection lines at the two different surfaces (Fig. 10) after their projection on the unit sphere $\mathbf{m}^2 = 1$ of propagation directions continue each other at the degeneracy points.

Topological transformations of wave surfaces and polarization fields create new features of the phenomenon of internal conical refraction. Still an extension of the theory may be done in terms of the same classic refraction cone bounded by the universal ellipse. As we have seen, in crystals without damping the classic picture of conical refraction automatically arises for a circularly polarized wave propagating along conical acoustic axis. In an absorptive crystal the same cone and universal ellipse as a trajectory of precession of the ray velocity vectors retain at the whole self-intersection line of the slowness surface between split degeneracy points.

Along singular axes the refraction does not differ from the classical picture: the isonormal waves degenerate into one circularly polarized wave with the ray precession of constant sectorial velocity $\overline{v}^{\text{sec}} = g\omega$ at the ellipse. A screen "illumination" related to such precession would look as a completely drawn ellipse (Fig. 15a). Some increase of intensity in the vicinity of large semi-axes $(S_{\max})$ is explained by a slower motion of the vector $\mathbf{s}_0$ in this region (its linear speed at the ellipse is equal $2\overline{v}^{\text{sec}} / S$). When the "observation" point passes along the ridge of the wedge to its middle, both the precession of the vectors $\mathbf{s}_{1,2}$ and the "illumination" pattern become less and less uniform (Fig. 15b,c). And in the center (ξ = 0) only two points (Fig. 15d) will turn to be "illuminated". They relate to the isonormal waves with linear polarization: the refraction becomes purely wedge-like. Thus, with scanning the ridge by the wave normal $\mathbf{m}$ the refraction continuously transforms from purely conic to purely wedge type.

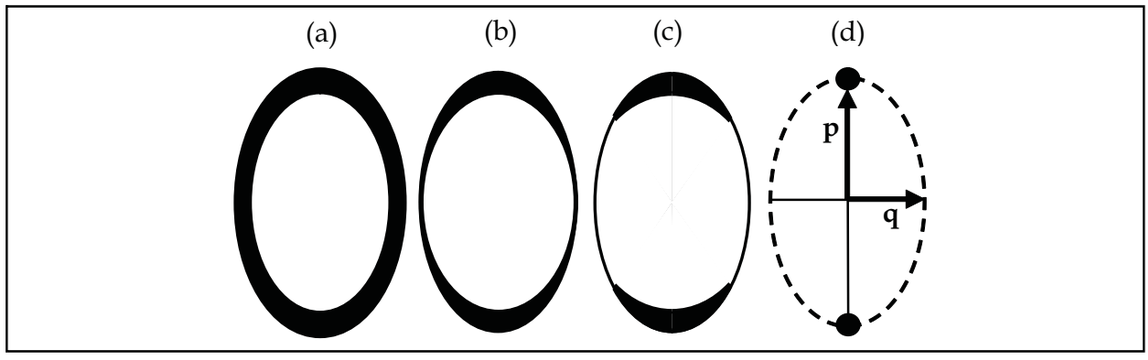

Fig. 15. Schematic plot of gradual transition from purely conical refraction (a) along a singular acoustic axis to purely wedge refraction in the middle of the ridge (d) for a particular case of the acoustic axis splitting from the symmetry plane

In conclusion, let us discuss the observability of the above beautiful and nontrivial physical effects. In principal, there is no threshold level of damping for the split of acoustic axes. Just the less damping, the less is the solid angle inside of which all the peculiarities manifest themselves. If this angle is less than the angle of the acoustic beam divergence, then we shall not observe neither splitting of acoustic axes, nor any accompanied effects. Thus, for the observability of our predictions the split angle $\delta\psi$ (46) must exceed the divergence of the beam. The best experimentally realizable collimation of sound beams is limited by the diffraction divergence, which is estimated as ~λ/d, where λ is the wave length and d is the diameter of the beam. So, with increasing frequency ω the angle $\delta\psi$ increases and the beam divergence, on the contrary, decreases. Thus, we deal here with a frequency threshold from below. The order of the splitting angle is determined by the estimate $\delta\psi = 2\delta m_0 \sim \omega\eta / \mu$ (46), where μ is the shear modulus and η is the viscousity. Substituting this estimate to the inequality $\delta\psi > \lambda / d$, one obtains the following lower threshold for the frequency $\nu = \omega/2\pi$

$$\nu > \nu_{\text{th}} \sim \sqrt{\frac{c_s \mu}{2\pi\eta d}}, \tag{107}$$

where c_s is the sound speed. There are known a series of physical mechanisms of the sound attenuation η. Often phonons play in it an important role. The phonon viscosity at room (or high) temperature T may be estimated as

$$\eta_{ph} \sim \tau_{ph}(3k_B T / a^3) . \tag{108}$$

Here τ_{ph} is the phonon relaxation time, k_B is the Boltzmann constant, and a is the lattice parameter. Substituting into eqns. (107), (108) $c_s \sim 3\cdot 10^5$ cm/s, $\mu \sim 10^{11}$ dyn / cm^2, $d \sim 0.5$ cm, $T \approx 300$ K, $a \sim 3\cdot 10^{-8}$ cm, $\tau_{ph} \sim 10^{-9}$ s, we come to the estimate $\nu_{th} \sim 100$ MHz. Thus, at rather high-frequencies, which however belong to experimentally available ultrasound range, the properties and effects described in this chapter appear quite observable.

10. Acknowledgment

Authors are grateful to A.L. Shuvalov for helpful discussions and to W. Gerulski for the help in computations related to the illustrations. The support of the Polish Foundation MNiSW (grant No N N 501252334) is gratefully acknowledged. V.I.A. is also grateful to the Kielce University of Technology for a hospitality and support.

11. References

Aleksandrov, K.S. & Ryzhova, T.V. (1964). Internal conical refraction of elastic waves in ammonium dihydrogen phosphate. *Kristallografiya*, Vol. 9, No. 3 (June 1964) 373-376, ISSN 0023-4761 [*Sov. Phys. Crystallography*, Vol. 9, No. 3 (1964) 298-300, ISSN 1063-7745]

Alshits, V.I. & Lothe, J. (1979). Elastic waves in triclinic crystals. *Kristallografiya*, Vol. 24, No. 4, 6 (Aug., Dec. 1979) 972-993, 1122-1130, ISSN 0023-4761 [*Sov. Phys. Crystallography*, Vol. 24, No. 4, 6 (1979) 387-398, 644-648, ISSN 1063-7745]

Alshits, V.I. & Lyubimov, V.N. (1998). Elastic waves in absorptive media: peculiarities of wave surfaces and singularities in the polarization fields. In: *Dissipation in Physical Systems,* A. Radowicz (Ed.), pp. 15-43, Politechnika Swietokrzyska, ISSN 0239-4979, Kielce. *Proceedings of 2nd Workshop on Dissipation in Physical Systems*, Borkow, Poland, September 1-3, 1997

Alshits, V.I. & Lyubimov, V.N. (2011). Conical refraction of elastic waves in absorptive crystals. *Zh. Eksp. Teor. Fiz.*, Vol. 140, No. 2(8) (Aug. 2011) [JETP, Vol. 113, No. 2 (2011), ISSN 1063-7761]

Alshits, V.I.; Sarychev, A.V. & Shuvalov, A.L. (1985). Classification of degeneracies and analysis of their stability in the theory of elastic waves in crystals. *Zh. Eksp. Teor. Fiz.*, Vol. 89, No. 3(9) (Sept. 1985) 922-938, ISSN 0044-4510 [Sov. Phys. JETP, Vol. 62, No. 3 (1985) 531-539, ISSN 1063-7761]

Barry P.A. & Musgrave, M.J.P. (1979). On elliptical conical refraction of elastic waves in tetragonal crystals. *Q. J. Mech. & Appl. Math.*, Vol. 32, No. 3 (March 1979) 205-214, ISSN 0033-5614

De Klerk, J. & Musgrave, M.J.P. (1955). Internal conical refraction of transverse elastic waves in a cubic crystal. *Proc. Phys. Soc. Lond. B*, Vol. 68, No. 2 (Feb. 1955) 81-88, ISSN 1088-0370

Fedorov, F.I. (1968). *Theory of Elastic Waves in Crystals*, Plenum Press, ISBN, New York

Khatkievich, A.G. (1962a). The acoustic axes in crystals. *Kristallografiya*, Vol. 7, No. 5 (Oct. 1962) 742-747, ISSN 0023-4761 [*Sov. Phys. Crystallography*, Vol. 7, No. 5 (1963) 601-604, ISSN 1063-7745]

Khatkievich, A.G. (1962b). Internal conical refraction of elastic waves. *Kristallografiya*, Vol. 7, No. 6 (Dec. 1962) 916-920, ISSN 0023-4761 [*Sov. Phys. Crystallography*, Vol. 7, No. 6 (1963) 742-745, ISSN 1063-7745]

Khatkievich, A.G. (1964). Special directions for elastic waves in crystals. *Kristallografiya*, Vol. 9, No.5 (Oct. 1964) 690-695, ISSN 0023-4761 [*Sov. Phys. Crystallography*, Vol. 9, No. 5 (1964) 579-582, ISSN 1063-7745]

Landau L.D. & Lifshitz, E.M. (1986). *Theory of elasticity*. Pergamon Press, ISBN, London

Musgrave, M.J.P. (1957). On an elliptic cone of internal refraction for quasi-transverse waves in tetragonal crystals. *Acta Crystallogr.*, Vol. 10, No. 4 (Apr. 1957) 316-318, ISSN

Shuvalov, A.L. (1998). Topological features of polarization fields of plane acoustic waves in anisotropic media. *Proc. R. Soc. Lond. A*, Vol. 454, (Nov. 1998) 2911-2947, ISSN 1471-2946

Shuvalov, A.L. & Chadwick, P. (1997). Degeneracies in the theory of plane harmonic wave propagation in anisotropic heat-conducting elastic media. *Phil. Trans. R. Soc. Lond. A*, Vol. 355 (Jan. 1977) 156-188, ISSN 1471-2962

Shuvalov, A.L. & Scott, N.H. (1999). On the properties of homogeneous viscoelastic waves. *Q. J. Mech. Appl. Math.*, Vol. 52 (Sept. 1999) 405-417, ISSN 0033-5614

Shuvalov, A.L. & Scott, N.H. (2000). On singular features of acoustic wave propagation in weakly dissipative anisotropic thermoviscoelasticity. *Acta Mechanica*, Vol. 140, No 1-2 (March 2000) 1-15, ISSN

Sirotin Yu.I. & Shaskolskaya, M.P. (1979). *Fundamentals of Crystal Physics* (in Russian), Nauka, Moscow [(1982) translation into English, Mir, ISBN, Moscow]

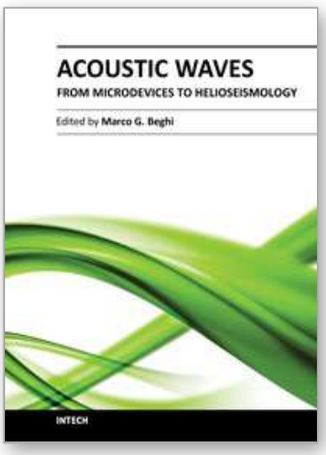

Acoustic Waves - From Microdevices to Helioseismology

Edited by Prof. Marco G. Beghi

ISBN 978-953-307-572-3
Hard cover, 652 pages
Publisher InTech
Published online 14, November, 2011
Published in print edition November, 2011

The concept of acoustic wave is a pervasive one, which emerges in any type of medium, from solids to plasmas, at length and time scales ranging from sub-micrometric layers in microdevices to seismic waves in the Sun's interior. This book presents several aspects of the active research ongoing in this field. Theoretical efforts are leading to a deeper understanding of phenomena, also in complicated environments like the solar surface boundary. Acoustic waves are a flexible probe to investigate the properties of very different systems, from thin inorganic layers to ripening cheese to biological systems. Acoustic waves are also a tool to manipulate matter, from the delicate evaporation of biomolecules to be analysed, to the phase transitions induced by intense shock waves. And a whole class of widespread microdevices, including filters and sensors, is based on the behaviour of acoustic waves propagating in thin layers. The search for better performances is driving to new materials for these devices, and to more refined tools for their analysis.

InTech Europe
University Campus STeP Ri
Slavka Krautzeka 83/A
51000 Rijeka, Croatia
Phone: +385 (51) 770 447
Fax: +385 (51) 686 166
www.intechopen.com

InTech China
Unit 405, Office Block, Hotel Equatorial Shanghai
No.65, Yan An Road (West), Shanghai, 200040, China
中国上海市延安西路65号上海国际贵都大饭店办公楼405单元
Phone: +86-21-62489820
Fax: +86-21-62489821

IntechOpen